THE SEA: THE SCIENCE OF OCEAN PREDICTION
Journal of Marine Research, 75, 263–300, 2017

Recent advances in nearshore wave, circulation, and sediment transport modeling

by James T. Kirby[1,2]

ABSTRACT

Significant advances in the modeling of nearshore processes have occurred over recent decades as a result of developments in both computational approaches and theoretical understanding. This review examines the present state of progress primarily from a hydrodynamics standpoint, followed by a brief discussion of applications to sediment transport and morphological evolution. Wave-averaged formulations of the wave-current interaction problem and resulting models for wave-induced currents are reviewed in order to compare and contrast radiation stress and vortex force approaches. Wave-resolving approaches are then discussed, with an emphasis on the recent rapid development of 3D nonhydrostatic models and their application to a wide range of physical problems. The recently developed understanding of the importance of vorticity generation mechanisms at wave-resolved scales, and their contribution to transport and mixing processes, are discussed.

Keywords: Boussinesq models, nearshore circulation, nonhydrostatic models, surf zone, wave-current interaction

1. Introduction

Modeling of the nearshore environment has come to a state of remarkable maturity in the last half-century, first through the introduction of wave-averaged forcing and resulting wave-driven flows and water level adjustments, and, more recently, wave-resolving models and an exploration of the effect of breaking wave geometry on mean flow vorticity dynamics. Useful formulations for wave forcing are based on either the radiation stress concept (Longuet-Higgins and Stewart 1960, 1962, 1964), in which forcing is expressed as the divergence of a stress tensor expressing excess wave momentum flux, or on the vortex-force, or CL formalism (Craik and Leibovich 1976), where wave forcing appears through a combination of terms expressing vortex force, divergence of wave volume flux, and the dissipation of wave energy. Although the radiation stress concept still serves as the primary pedagogic tool in explaining nearshore processes, vortex force formalism clearly

1. Center for Applied Coastal Research, Department of Civil and Environmental Engineering, University of Delaware, Newark, DE 19716, USA.
2. Corresponding author: ***e-mail: kirby@udel.edu***

identifies the central role played by wave energy dissipation in providing a driving force for wave-averaged flows, thereby providing a natural indication of the identity of the surf zone as the region where dissipation dominates over other forcing mechanisms. Both formalisms have been, or could be, used to provide the basic description of a range of basic surf zone processes, including wave set-up, alongshore currents, and rip currents. Simple process models are skillful in reproducing basic surf zone behavior in suitably simple settings, and more generalized models that describe wave-induced circulation over arbitrary bathymetry are widely available. Wave forcing is now routinely implemented in more general ocean circulation models for application from the deeper ocean to the shoreline.

More recently, exploration of the capabilities of the existing wave-averaged formulations has led to a growing awareness of the significant limitations of this approach. At smaller scales, models for wave-driven nearshore circulation utilizing wave-averaged formulations can strongly underpredict the energetics of wave-scale vorticity and associated mixing effects. This underprediction results from the absence of vorticity-producing mechanisms associated with localized dissipation in finite-length breaking wave crests, which are absent after wave averaging reduces dissipation to a smooth structure on the scale of the surf zone width. At larger scales, hydrostatic models for circulation can fail to resolve critical mechanisms such as frontal formation or interfacial instabilities in strongly stratified inlets and coastal regions. This leads to less than satisfactory predictions of waves and currents that control sedimentary processes in these environments.

At present, fixes for these limitations typically lead away from a common framework in multiple directions, reducing the potential for a uniformly applicable model system. At small scales, the problem of wave-scale forcing can be addressed using the well-developed class of Boussinesq models. These models resolve individual wave crests and the structure of breaking events, but are difficult to extend to a wider range of physical settings without introducing model equations that can defy simple understanding. In the more generalized nearshore ocean environment, nonhydrostatic circulation models resolve problems associated with certain baroclinic processes, but leave unanswered the problem of the spatial distribution of breaking and its contribution to the generation of fine-scale vorticity. In particular, the use of a stochastic distribution of breaking events in deep water, based on observational knowledge of the distribution of whitecap events as a function of wind speed, has no counterpart to address depth-limited breaking over complex bathymetry in the nearshore.

The strengths and weaknesses of the wave-averaged formalism are here reviewed in the context of the present state of modeling wave, current, and sediment transport processes in the nearshore ocean. The role of wave-resolving models in improving understanding in these various areas is discussed. A number of other recent articles provide a wide range of information on specific topics that are covered only briefly or ignored here, including Dalrymple et al. (2011) on rip currents, Ribas et al. (2015) on coastal morphology, and Monismith (2007) on coral reef hydrodynamics.

2. Modeling approaches

Variations in approaches to developing different classes of nearshore models can be explained starting from the three-dimensional (3D), Reynolds-averaged Navier-Stokes (RANS) equations for incompressible flow of constant density, written in tensor notation as

$$\frac{\partial q_i}{\partial x_i} = 0 \tag{1}$$

$$\rho\left(\frac{\partial q_i}{\partial t} + q_j \frac{\partial q_i}{\partial x_j}\right) + \frac{\partial p}{\partial x_i} = \frac{\partial \tau_{ij}}{\partial x_j} - \rho g \delta_{i3} \tag{2}$$

where indices i, j range over values 1, 2, 3 denoting x, y, z, with z pointed upwards against gravity g. q_i, τ_{ij}, p and ρ denote velocity, the turbulent stress tensor, pressure, and density, respectively. The models considered below often employ a depth-integrated version of equations (1) and (2), but these depend to some extent on the theoretical context and choice of numerical approach, and are mentioned only as needed. The velocity vector q_i has formally been averaged over turbulent length and/or time scales, with the resulting turbulent stresses given by

$$\tau_{ij} = -\rho\langle q_i' q_j' \rangle, \tag{3}$$

where primes denote turbulent quantities. q_i retains all information about motions at the scale of organized wave motion as well as lower frequency motions down to and including the steady flow limit. The modeling approaches considered here include wave-resolving formulations, where the entire organized flow field q_i is solved for simultaneously, and wave-averaged formulations, where the velocity vector is separated into wave and slowly varying current components

$$q_i = \tilde{q}_i(x_i, t) + \overline{q}_i(x_i, t), \tag{4}$$

where the current field $\overline{q}_i$'s dependence on space and time is assumed to be slow enough to allow for an adequate averaging over more rapidly varying wave motions. Introduction of (4) in Equations (1)–(2) and averaging leads to a model for the current field with added wave forcing terms; these terms are specified, in turn, through the use of an external model for the wave behavior.

Either category of models exists in depth-integrated, 2D horizontal form (with possible extensions to account for vertical flow structure in a semianalytic fashion, leading to Quasi-3D models), or full 3D form.

3. Wave-averaged formulations

Historically, wave-averaged models have provided the backbone for developing physical understanding of wave-driven processes in the nearshore ocean. Such models are derived by substituting (4) into (1)–(2) and then averaging over suitable length or time scales to

eliminate rapid wave fluctuations from the equations for the slowly varying current field. Averaging can be carried out in the 3D equations or after depth-integration. Two classes of model are in present use; models employing the radiation stress formulation (Longuet-Higgins and Stewart 1960, 1962, 1964), or CL models, which are based on the vortex-force formulation introduced by Craik and Leibovich (1976).

Inherent to both approaches is a two-step interaction, in which mean flows result from wave forcing (the WEC, or wave-effect-on-current step), and in which currents modify the structure of the wave field (the CEW, or current-effect-on-waves step). Early examples of circulation modeling often neglected the second step, assuming CEW are small for current speeds significantly less than wave phase speed. The approach is more economical and doesn't require close coupling between circulation and wave models; see Allen et al. (1996), Slinn et al. (1998), and Özkan-Haller and Kirby (1999) for representative examples. However, a number of recent studies have shown that the feedback from currents to waves has a significant impact on the resulting wave forcing and circulation pattern, indicating that coupling must be represented properly. These results have been seen in early studies on alongshore current instabilities (Özkan-Haller and Li 2003) and rip currents (Yu and Slinn 2003) based on radiation stress formulations, and, more recently, in additional research on rip currents (Weir et al. 2011) using the CL approach, where the relative importance of dissipation and conservative interactions is addressed.

a. Radiation stress

A physically based understanding of nearshore wave and current processes began to develop in the 1960s in response to the development of the concept of the radiation stress and its application in 2D depth-integrated circulation models (Longuet-Higgins and Stewart 1960, 1964). In analogy to the development of the Reynolds stress after averaging over turbulent length scales, radiation stress arises after manipulating advective accelerations according to

$$q_j \frac{\partial q_i}{\partial x_j} = \frac{\partial q_i q_j}{\partial x_j} - q_i \frac{\partial q_j}{\partial x_j}, \tag{5}$$

where the second term on the right is identically zero, and then averaging over wave scales after substituting (4) to obtain a stress-like term resulting from wave momentum flux analogous to (3). The resulting wave-based second-order correlations may be expressed in terms of wave energy density E, which is supplied through solution of the wave energy or wave action equation. Longuet-Higgins and Stewart (1963) first used the formulation to explain the phenomenon of wave setup, leading to a superelevation of the mean shoreline on the beach face resulting from a balance between an onshore force resulting from the shoreward decay of wave momentum flux, and an offshore force maintained by the pressure gradient force resulting from the tilt of the mean water surface. This phenomenon was further considered by Bowen et al. (1968). In the case of oblique wave incidence, Bowen (1969b),

and Longuet-Higgins (1970a, b) showed that a mean current, directed in the alongshore-direction, results from the development of a mean bottom stress directed against the force resulting from the shoreward decay of alongshore-directed wave momentum flux. Finally, Bowen (1969a) considered the forcing of surf zone circulation resulting from alongshore periodic variations in wave forcing, and showed that circulation cells or rip currents would be set up in response.

The early explication of setup, alongshore current, and rip currents using the radiation stress concept represented a major step forward in understanding basic surf zone processes. The results pointed out the singular importance of wave-breaking dissipation, although dissipation itself is expressed in the basic formulation only through the pattern of decaying wave height. Indeed, these early canonical results, based on a similarity assumption of unchanging wave height to water depth ratio across the surf zone, would imply patterns of wave energy dissipation that are realistic in a very limited set of circumstances. More realistic formulations, depending on the application of the full action balance equation for nearly monochromatic waves (Bretherton and Garrett 1968) or elaborate spectral evolution models (Booij et al. 1999) applied over realistic bathymetry, produced a range of models that exhibited increasing skill in describing nearshore flows when tested against data. Consideration of the effect of vertical variation in mean currents on depth-averaged momentum flux leads to the development of a stress tensor that provides a significant mixing mechanism for momentum (Svendsen and Putrevu 1994; Putrevu and Svendsen 1999) and passive scalars (Smith 1995), in analogy to the Taylor dispersion mechanism in turbulent pipe flow (Taylor 1953; Elder 1959). This approach provides the basis for Quasi-3D models (Haas et al. 2003), where the tensor is evaluated semi-analytically using local, linearized solutions for the momentum balance.

Early 3D wave-averaged models were usually formulated in terms of radiation stresses as well, but with some degree of difficulty in determining the vertical structure of forcing. Mellor (2003, 2008) has contributed to the further development of formulations for radiation-stress-based forcing; these formulations have been employed in a number of models (Warner et al. 2008, 2010; Kumar et al. 2011). Haas and Warner (2009) provide an early example of a comparison of Quasi-3D and 3D model results in the limited setting of a simple alongshore current; see also Kumar et al. (2011). It is generally the case, though, that the concept has maintained a weakening foothold in the 3D model setting; it is losing ground to the vortex-force or CL formalism.

Dingemans et al. (1987) pointed out that radiation stress formulations, in which forcing is obtained by differentiating a potentially already unsmooth estimate of the stress tensor, can be difficult to stabilize in application to complex settings. Seeking an alternative, Dingemans et al. developed a rearrangement of the forcing terms, leading to a form that explicitly identifies wave dissipation as an isolated component, and that was shown to be by far the most important component of forcing in the surf zone. A separate approach to this problem, yielding a similar indication of the dominance of dissipation in driving surf zone flows, was provided by Bühler and Jacobson (2001). This reduced form of radiation stress forcing,

with extensions to describe depth-dependence, forms the basis for the WEC component in the popular model, Delft-3D (Lesser et al. 2004). These formulations implicitly leave out forcing effects in the presence of unbroken waves, and would not, for example, be expected to describe the broadening of jets in the presence of an opposing train of unbroken waves (Ismail and Wiegel 1983).

b. Vortex force

The formulation of Craik and Leibovich (1976) is explained schematically by the alternate treatment of advective acceleration, given more conveniently in vector form by

$$\mathbf{q} \cdot \nabla \mathbf{q} = \frac{1}{2} \nabla (\mathbf{q} \cdot \mathbf{q}) + \mathbf{q} \times \omega, \tag{6}$$

where $\omega = \nabla \times \mathbf{q}$ is the fluid vorticity. Advective acceleration then becomes the combination of a pure gradient, representing the conservative effect of a Bernoulli head, which combines in a natural way with the pressure, and a vortex force, which acts in a direction perpendicular to the tangent plane formed by the velocity and vorticity vectors. Wave-averaged formulations in 3D, or further depth-integrated to 2D, are both expressed in forms that have fairly straightforward physical interpretations when considered in the context of the actual flow. The wave-forcing terms in depth-integrated 2D flow may be written as

$$\mathbf{F}_w = D_w \mathbf{k} + \mathbf{Q}_s \times \mathbf{\Omega} - \mathbf{U} \nabla_h \cdot \mathbf{Q}_s - H \nabla_h J \tag{7}$$

(Smith 2006; Uchiyama et al. 2009). The first term on the right expresses a force proportional to the rate of energy (or wave momentum) decay D_w projected in the direction of the wavenumber vector $\mathbf{k}$, and is equivalent to the portion of radiation stress retained by Dingemans et al. (1987) and subsequently used in Delft 3D (Lesser et al. 2004). The second term is the vortex force, expressed as the curl of the horizontal Stokes drift (or mean wave momentum) $\mathbf{Q}_s$ and the vertical vorticity vector $\mathbf{\Omega}$ representing the curl of the horizontal, depth-averaged velocity $\mathbf{U}$, leading to a force acting at right angles to the wavenumber vector aligned with $\mathbf{Q}_s$. This term represents the reaction to wave refraction, in which the direction of wave momentum is changed, resulting in the appearance of an equal and opposite force exerted on the mean flow. The third term expresses the force associated with the increase or decrease of Stokes drift (interpreted as wave mass flux). The final term is a conservative contribution leading to wave setdown, with H being wave-averaged water depth and J being identical to the pressure contributions to the radiation stress. A complete explication of the 3D theory may be found in McWilliams et al. (2004) and Ardhuin et al. (2008).

The vortex force formulation has become an important part of coastal modeling and is, at present, probably the dominant means of expressing wave forcing in 3D models. A number of practical implementations have been developed (Newberger and Allen 2007; Uchiyama et al. 2010; Kumar et al. 2012), based on formulations developed by McWilliams et al. (2004) and Ardhuin et al. (2008).

c. Strengths and weaknesses of each approach

For the case of depth-integrated flows, Smith (2006) has demonstrated the equivalence of radiation stress and vortex force formulations by providing the derivation of one from the other. This equivalence was demonstrated numerically by Shi et al. (2006), who showed equivalent results when both models were run with continuous coupling between currents and waves (WEC+CEW). Interestingly, this equivalence breaks down when coupling is updated only intermittently, with a clear indication that the vortex force model retains better accuracy with progressively weakened coupling. This result was thought to be related to the form of the vortex force term, which can utilize the updated current field and thus partially maintains continuous coupling during time-stepping of the circulation model, even if corresponding updates to the Stokes drift are not available.

The CL formulation, applied to both dissipative and non-dissipative situations, often offers a simple intuitive explanation of observed phenomena, such as the formation of a current jet flowing in the direction of waves during wave breaking over a mound (Mulligan et al. 2010), or the rapid startup of the seaward-directed rip in gaps in alongshore bars. In some instances, the CL formulation provides a clear explanation of phenomena that are not easily explained using radiation stress-based arguments, such as the slowing and broadening of a jet opposing a wave field in the absence of breaking (Ismail and Wiegel 1983), where Yoon and Liu (1990) concluded that the conservative interaction of jet and opposing current should actually lead to a narrowing and intensification of the jet. In contrast, the second term in (7), which represents the dominant component of wave forcing in the absence of wave breaking, clearly indicates that the tendency of the jet to refract waves towards the jet axis leads to a force exerted on flow in the jet in the direction away from the jet axis, leading to broadening of the jet and, by continuity, relative slowing of the centerline jet velocity.

Possibly the main drawback to use of the CL formulation across the board is the fact that the classical literature and textbook formulations have generally explained the basic aspects of surf zone flows using the radiation stress formulation. There is a need for a detailed textbook explication of the range of classic problems including set-up, longshore current, and rip current dynamics using the CL approach.

Finally, models such as Delft-3D, in which the radiation stress forcing is reduced essentially to a form corresponding to the first term in (7) resulting from wave breaking, would neglect the conservative component of wave-current interaction. This loss was initially thought to be unimportant (Dingemans et al. 1987); however, further studies of the relative importance of the various forcing effects (Weir et al. 2011) show that the vortex force component of wave forcing plays a significant role in determining current patterns, such as rip currents, that extend to or beyond the nominal surf zone boundary.

4. Wave-resolving models

The advent of significantly more powerful computers in recent decades makes it possible to carry out phase resolving simulations of surface and internal wave motions over physical

length scales that are extensive enough to provide a comprehensive picture of nearshore processes. The main computational approach for carrying out these studies has been based on the theory for weakly dispersive waves pioneered by Joseph Boussinesq in the late 1800s (Boussinesq 1872). The growth in development and application of Boussinesq Type Models (or BTMs) has been explosive, with simulations of surface wind waves over domains with dimensions of tens of kilometers now being readily feasible. Recent reviews on the topic may be found in Brocchini (2013) and Kirby (2016).

More recently, fully 3D models for coastal processes are coming into common usage. Three-dimensional modeling can take on a wide range of meanings, with the high-resolution extreme involving detailed modeling of turbulent flows and complex water surfaces using Volume-of-Fluid (VOF) or level set models on fixed grids, meshless Lagrangian particle methods such as Smooth Particle Hydrodynamics (SPH), or a range of other modern candidates. At the opposite extreme, there is increasingly the desire to allow for arbitrary vertical flow structure and large vertical acceleration effects, but without the need to obtain or utilize horizontally varying spatial information at scales that are any finer than already provided by the Boussinesq model being replaced. This latter class of model has come to be referred to as the nonhydrostatic model.

a. Boussinesq, Serre, and Green and Naghdi models

Boussinesq Type Models such as Boussinesq, Serre, or Green and Naghdi models are typically thought of as being models for weakly dispersive motion, where wave-induced horizontal flow deviates little from vertical uniformity and where vertical acceleration effects are weak. Scaling arguments originally used for models of this type, which also includes the one-way model of Korteweg and de Vries (1895), are based on the assumption of weak nonlinearity, characterized by

$$\delta = \frac{a_0}{h_0} \ll 1, \tag{8}$$

where a_0 characterizes wave amplitude and h_0 characterizes still water depth, and on weak dispersion, characterized by

$$\mu = \frac{h_0}{\lambda_0} \ll 1, \tag{9}$$

where λ_0 represents a scale for wave length. The theory then results from retention of the leading order effects of nonlinearity and dispersion, which appear at $O(\delta)$ and $O(\mu^2)$, with the Ursell number $\delta/\mu^2 = O(1)$. Recent derivations of models of this type often impose no restriction on the size of δ, which becomes a placeholder in the nondimensional equations (Serre 1953; Green and Naghdi 1976; Wei et al. 1995; Chen 2006). Models of this type are usually referred to as being fully nonlinear.

Allowing the wavenumber k to represent the inverse of a wavelength scale allows the parameter μ to be written as $\mu = kh$. The role of this dispersion parameter is made clear by

examining the Taylor series expansion of the linear wave dispersion relation for kh about the shallow water limit $kh = 0$,

$$\omega^2 h/g = kh \tanh kh = kh\left(kh - \frac{1}{3}(kh)^3 + \frac{2}{15}(kh)^5 + \cdots\right) \tag{10}$$

Shallow water theory results from the neglect of all but leading order terms, giving a dispersion relation

$$\omega^2 = ghk^2 \tag{11}$$

with a resulting phase speed $c = \omega/k = \sqrt{gh}$ that does not depend on frequency ω. The model equations that correspond to this limit are referred to as the nonlinear shallow water equations, or NLSWE. The classic theory described by Boussinesq (1872) hinges on retention of one further term and leads to models that are asymptotically equivalent to

$$\omega^2 = ghk^2\left(1 - \frac{1}{3}(kh)^2\right), \tag{12}$$

and which are referred to as being weakly dispersive. The appearance of the leading order dispersion correction at $O(\mu^2)$ is clear. Modern extensions of the theory revolve around the effective rearrangement of the truncated series to improve accuracy (using techniques such as Padé approximants), the extension of the series to higher order, and the combination of both. Brocchini (2013) and Kirby (2016) provide thorough reviews of this development. The second parameter δ represents the ratio of a characteristic wave amplitude a_0 to depth h_0, and thus represents the degree of nonlinearity in the problem. The classical theory and modern extensions have played a key role in the understanding of wave propagation and in the development of models that are useful for both scientific discovery and engineering application. Modern-day models incorporate a wide range of extensions to account for additional physical effects that lie outside of the range of the original formulation for inviscid, irrotational flow. There is an extensive literature on the application of the model to coastal engineering problems such as harbor oscillation (Lepelletier and Raichlen 1987), morphology adjustment (Karambas and Koutitas 2002; Xiao et al. 2010; Kim 2015), and breakwater and reef overtopping and coastal inundation (Lynett et al. 2010; Roeber and Cheung 2012; Li et al. 2014).

Various versions of BTM models exist in the literature. A velocity-based BTM retaining terms to $O(\mu^2)$ may be written as a two-equation system for surface displacement η and a horizontal velocity $\mathbf{u}$, which represents either a depth-averaged value (Peregrine 1967) or a value at a reference depth (Nwogu 1993), given by

$$\eta_t + \nabla_h \cdot \mathbf{M} = 0 \tag{13}$$

$$\mathbf{u}_t + \delta\mathbf{u} \cdot \nabla_h \mathbf{u} + \nabla_h \eta + \mu^2(\mathbf{V}_1 + \mathbf{V}_2 + \overline{\mathbf{V}}_3) = O(\mu^4), \tag{14}$$

where $\mathbf{M}$ is depth-integrated volume flux or momentum, and where $\mathbf{V}_1$, $\mathbf{V}_2$, and $\overline{\mathbf{V}_3}$ represent dispersive effects resulting from the vertical structure of horizontal velocity and the presence of a nonhydrostatic correction to the wave-induced pressure field. BTM models may deviate from the form illustrated here due to choice of dependent variables, and it is now common to prefer a flux form of (14) over the velocity form illustrated to facilitate model implementation in finite-volume schemes based on conservation laws (Shi et al. 2012; Kim et al. 2009; Bonneton et al. 2011a, b).

b. Three-dimensional wave-resolving, nonhydrostatic models

Development of higher-order Boussinesq models and their extension to cover a more complete set of physics leads to a rapid increase in model complexity, as evidenced by the first simple extension from $O(\mu^2)$ to $O(\mu^4)$ models for ideal fluids (Gobbi et al. 2000). In addition, the vertical structure of physical effects such as boundary layer turbulence or the profile of transported scalars may not be simple to parameterize in regions of more rapidly varied flow, which poses a possible limit to the potential accuracy of depth-integrated equations. As a result, there has been a great deal of recent interest in the development of a new category of free-surface models that retain the relative efficiency of depth-integrated solvers and provide access to a fully 3D determination of flow characteristics when needed.

Nonhydrostatic models are basically an approach to solving the RANS equations (1)–(2) (or, in some cases, a more highly resolved LES model) using simplified free surface boundary conditions that are consistent with the resolution usually used in the depth-integrated BTM models. Work in this direction was initiated mainly by Casulli and Stelling (1998) and Casulli (1999), with subsequent contributions from a number of research groups (Stelling and Zijlema 2003; Yuan and Wu 2004; Bradford 2005, 2011; Young et al. 2007; Zijlema and Stelling 2008). At least two readily accessible open-source models have been developed: SWASH (Zijlema et al. 2011) and NHWAVE (Ma et al. 2012).

Nonhydrostatic models provide a robust means for computing a wide range of phenomena in the coastal ocean. The models gain their efficiency from a combination of several factors. First, acceptance of the idea that the surface will not be reproduced at higher resolution than used in Boussinesq models leads to the adoption of a locally smooth, single-valued representation. This allows the mass conservation equation to be integrated over depth in order to specify the surface location in terms of the divergence of volume flux, as in (13). The approach differs from Boussinesq theory, however, in retaining the 3D momentum equations. For the case of surface wave propagation in homogeneous inviscid fluids, model results usually show good agreement with experimental results using as few as three or four discretization levels in the vertical (Ma et al. 2012). The most time-consuming aspect of the numerics, as in most Navier-Stokes solvers, is the solution of a Poisson equation for the nonhydrostatic pressure correction, which makes the model more expensive to run than BTMs even in the ideal fluid case. However, available Poisson solvers (such as HYPRE) are highly developed and scale well in multi-processor, distributed memory environments. As a result, extensions to physical formulations and the numerical development of this class of model,

which lacks the higher derivative terms common to all BTMs, is actually simpler and more transparent than in the Boussinesq approach. The models are easily extended to incorporate additional physical effects by the addition of scalar transport equations and adjustment of surface and body force expressions. For example, NHWAVE has been extended to account for suspended sediment load (Ma et al. 2014), interaction with submerged plant canopies (Ma et al. 2013b; Wu et al. 2016), landslide tsunami generation by dispersed gravity flows (Ma et al. 2013a) and layer-averaged granular debris flows (Ma et al. 2015), and interaction with floating bodies such as ice floes (Orzech et al. 2016). For motions with baroclinic effects in the form of density stratification, or significant vertical variations in obstacles such as plant canopies, it is often necessary to use higher vertical resolution to obtain an accurate description of the velocity field. A comparable increase in resolution in the solution for the pressure field can impose excessive computational burden, however, through simple growth in size of the matrix for the discretized Poisson equation, and through increasingly poor conditioning of that matrix. Strategies have been developed in which the nonhydrostatic pressure is solved for on a grid with much lower vertical resolution, and then interpolated back to finer resolution for use in the momentum equations (van Reeuwijk 2002; Shi et al. 2015b). Wave breaking is handled naturally in the calculation, and studies have verified nonhydrostatic models' ability to correctly reproduce regular and random wave breaking and infragravity wave generation effects (Ma et al. 2012; Smit et al. 2013, 2014; Rijnsdorp et al. 2015). The details of wave breaking computations in these models are still not well understood, however, particularly the partitioning between numerical dissipation and physical dissipation due to resolved turbulent diffusion terms.

Nonhydrostatic models are considerably more computationally intensive to run than BTM models due to resolution of the velocity field on multiple vertical levels, and the use of an elliptic pressure-Poisson equation to resolve the nonhydrostatic correction to the pressure field. This latter component of the solution often requires the installation of specialized packages on the computer system in use. Models are also often formulated in a σ coordinate system, where water surface and bottom are assumed to be single valued (as in NLSWE or BTM models) and are mapped onto flat surfaces, with $\sigma = (h + z)/(h + \eta)$ varying from $0 \leq \sigma \leq 1$. Velocity values saved at fixed σ levels during a computation thus have a semi-Lagrangian character, and mapping values onto fixed Eulerian z coordinates presents an added difficulty.

c. Turbulence-resolving models: LES and SPH

In addition to the nonhydrostatic models discussed above, use is often made of more conventional Navier-Stokes solvers based on the RANS equations (1)–(2) (Lin and Liu 1998) or on subgrid-scale-averaged Large Eddy Simulation (LES) models (Lakehal and Liovic 2011). Models have recently been extended to cover multiphase flows including fine sediments (Ozdemir et al. 2011) and entrained bubbles (Ma et al. 2011; Derakhti and Kirby 2014) using polydisperse continuum models, where discrete particles are treated in terms of a probability density function representing volumetric concentration. These

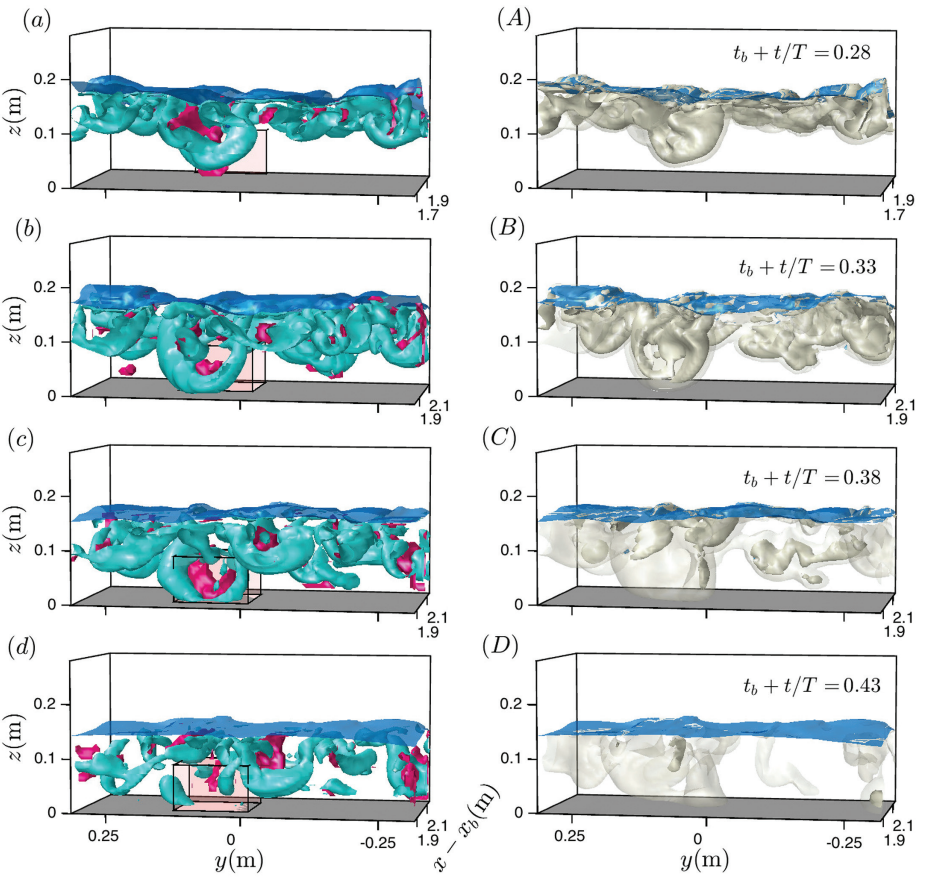

Figure 1. (right) Coherent structures or eddies (blue) and low-vorticity turbulent patches (red), and (right) void fraction contours indicating location of bubble clouds under a surf zone breaking wave crest. Coherent structures identified using the Q criterion of Hunt et al. (1988) (after Kirby and Derakhti (2015)).

models typically are formulated using finite-volume approaches, with irregular free surfaces modeled using volume-of-fluid (VOF) or level set approaches. Figure 1 shows a sample multiphase computation for bubble entrainment and transport under a surf zone-breaking wave crest. The left panel shows turbulent coherent structures identified using the Q criterion (blue) (Hunt et al. 1988), with a downward-translating horseshoe eddy prominent just left of center in the frame. Regions of high turbulence but small organized vorticity are shown in red and are usually associated with the ejected fluid driven between the legs of the horseshoe vortex. Similar organization of the flow field is seen in 3D PIV observations in the lab; the pink box in the left frame shows the size of a region corresponding to measuring volumes described in Ting and Reimnitz (2015). The right panel shows the spatial distribution of

entrained air, illustrating the combined effects of trapping within organized vortex cores and downward transport as part of the highly turbulent ejected volume. These modes of transport account for essentially all of the net downward component of air transport under the breaking crest.

In addition to grid-based LES, DNS, or RANS schemes, gridless Lagrangian schemes such as smooth particle hydrodynamics (SPH) have become popular in recent years, and represent an efficient approach to detailed fluid dynamic computations due to their relatively straightforward implementation on Graphical Processor Unit (GPU) computer architectures (Monaghan and Kos 1999; Dalrymple and Rogers 2006). Farahani and Dalrymple (2014) have reported SPH calculations of turbulence and coherent structures under breaking solitary waves crests, which compare well with laboratory data and are numerically efficient relative to typical LES and VOF calculations on conventional computers.

5. Wave breaking

Accurate modeling of the nearshore depends on the ability of the model being used to represent the spatial pattern of wave evolution and breaking wave decay with fidelity. This requirement is generally satisfied to the degree required in wave-resolving models, while the absence of a representation of breaking in individual wave crests presents a limitation for wave-averaged models that is becoming more pronounced, as discussed below.

a. Wave-averaged approaches

The principal step beyond the unphysical similarity form for breaking waves employed in early radiation stress-based studies is to use a physics-based model for dissipation in individual bores. Using the analogy to a traveling hydraulic jump or bore front, Divoky et al. (1970) formulated a model for the rate of dissipation in a propagating, breaking wave crest. Popular extensions of this approach to stochastic versions for random waves, incorporating probability of breaking for a distribution of wave heights, include the models of Battjes and Janssen (1978) and Thornton and Guza (1983). These models, along with more highly tuned modern variants, generally are expected to predict wave height distributions with errors of less than 10% (Apotsos et al. 2008). The introduction of the wave-roller energy balance, which transfers energy from breaking wave to organized roller motion at the onset of breaking and thus delays transfer to turbulent dissipation and resulting mean motions or surface displacements, further improved the description of forcing by introducing a spatial lag between the first occurrence of breaking and the onset of dissipation-driven responses (Stive and De Vriend 1994).

b. Wave-resolving simulations

Wave breaking in wave resolving models may be introduced either through explicit application of a damping effect in the governing equations, or by the temporary suppression of dispersive effects leading to shock formation. Explicit models for breaking wave dissipation

include roller models (Schäffer et al. 1993), detailed vorticity models (Veeramony and Svendsen 2000) or eddy viscosity models (Zelt 1991; Kennedy et al. 2000; Cienfuegos et al. 2010); the latter remain most popular today (Kirby 2016). Most recent progress has been made using a hybrid approach, where dispersive effects are turned off when some criterion is reached, reducing the BTM to the nonlinear shallow water equations (NLSWE). Already steep wave crests rapidly evolve towards discontinuous jump solutions, which are characteristic of the NLSWE, and lead to energy dissipation rates that are consistent with the theory for hydraulic jumps or bores with comparable crest-to-trough surface elevation changes. The approach, which appears to have been introduced by Tonelli and Petti (2009), goes hand in hand with the adoption of the finite volume method as the dominant computational approach, since these methods had already evolved to provide robust, shock-capturing capabilities for the NLSWE (Toro 2001). Since the consequence of turning off dispersion and shifting to the NLSWE form is basically the same in any robust solution method for the NLSWE, the differences between implementations of the strategy basically boils down to choosing criteria for (1) when to turn dispersion off and (2) when to turn it back on. Examples of the application of this hybrid approach may be found in Tonelli and Petti (2010, 2011, 2012), Shi et al. (2012), Roeber and Cheung (2012), Tissier et al. (2012), among others.

6. Wave-driven currents

Given appropriate boundary conditions and within the limitations of the depth-averaged flow field description, Boussinesq models provide a calculation of the entire flow field. Yoon and Liu (1989) first derived a coupled wave-current system based on Boussinesq scaling. Equivalent systems of equations can be obtained directly from a Boussinesq model, but the model must be a fully nonlinear type. Comparable derivations, starting from weakly nonlinear models and using a decomposition of velocity into wave and current components, lead to defective sets of coupled equations, indicating that the wave driven mean flows may be of suspect accuracy. There are as of yet no detailed model intercomparisons of weakly nonlinear vs. fully nonlinear models and comparison to data that would substantiate this claim, and it is assumed for now that weakly nonlinear and fully nonlinear BTMs are equally valid predictors of surf zone dynamics.

Boussinesq type models have been extensively used to study the large scale structure of surf zone flows. Chen et al. (1999) conducted a study of rip currents generated by segmented laboratory bars. Chen et al. (2003) developed an improved representation of modeled vertical vorticity effects, and applied the model in a study of alongshore currents during the DELILAH field experiment at Duck, NC. This study revealed the growth to finite amplitude and breakdown of shear waves, and showed that alongshore pressure gradients can play a significant role in the alongshore momentum balance over beaches with fairly weak alongshore variations. Additional comparisons of wave-averaged circulation and model-predicted wave statistics may be found in Feddersen et al. (2011), Geiman et al. (2011), Feddersen (2014), and Choi et al. (2015).

a. Short-crested incident waves

Since the work of Peregrine (1998), who studied the impulsive generation of vertical vorticity occurring along a breaking wave crest with along-crest wave height variation, it has become clear that a major source for vorticity generation in the wave-driven ocean is associated with detail at the scale of the wave crest. In the deep ocean, this additional contribution to vorticity generation is associated with the pattern of whitecaps on the surface and the scale of the individual breaking events. This contribution can be successfully treated using stochastic representations (Sullivan et al. 2007), since the spatial coverage of whitecaps is uniformly distributed and the scales of variation of the wind forcing are large relative to the scales associated with distance between whitecap events. The addition of this stochastic component of forcing leads to significant changes in levels of upper ocean turbulence, transport by Langmuir circulation, and mixed layer deepening. In contrast, the nearshore environment is complex in ways that would likely defy the successful development of a purely stochastic forcing model. The surf zone scale is small in contrast to the scale of the pattern of breaking dissipation. The location and structure of breaking can be controlled as much by the pattern of inhomogeneities in depth as by intrinsic short-crestedness in the waves themselves. Clark et al. (2012) performed a detailed study of vorticity generation at the scale of breaking wave crests, verifying that the predictions of Peregrine (1998) are correct. However, the likelihood of developing a simple stochastic extension to the smoother wave forcing fields that are characteristic of wave-averaged models seems remote, given the inevitable interplay of the intrinsic short-crestedness of the incident wave field and its interaction with a similarly variable underlying bathymetry. (An approach to this problem may possibly be found, however, in spectral models that account for finite de-correlation distances in wave statistics, and which thus have some ability to represent short-crested wave patterns induced by bottom geometry (Smit et al. 2015)).

Wave-resolving models, on the other hand, retain a complete description of crest geometry and the pattern of wave energy dissipation resulting from breaking. A number of studies have utilized BTMs to examine small-scale forcing and resulting flow field turbulence and horizontal mixing effects. In a pioneering study, Johnson and Pattiaratchi (2006) simulated directional random waves incident on a plane beach. They clearly demonstrated the presence of vorticity generation during the passage of breaking wave crests, and they further demonstrated the tendency for fine-scale vorticity, accumulated in the nearshore, to organize into larger-scale structures and finally to transient rip currents (Fig. 2). Spydell and Feddersen (2009) showed that BTM with directionally spread waves generated a rich vertical vorticity field with eddies at a range of length-scales and that the dispersion of numerical drifters was consistent with observations. Feddersen et al. (2011) and Clark et al. (2011) extended the comparison of BTM results and field observations to the case of obliquely incident waves in order to obtain estimates of both cross-shore and alongshore diffusivities. Feddersen (2014) and Choi et al. (2015) examined strong alongshore flows observed during the SandyDuck experiment in 1997. Feddersen compared results of a BTM model with resolved short-scale

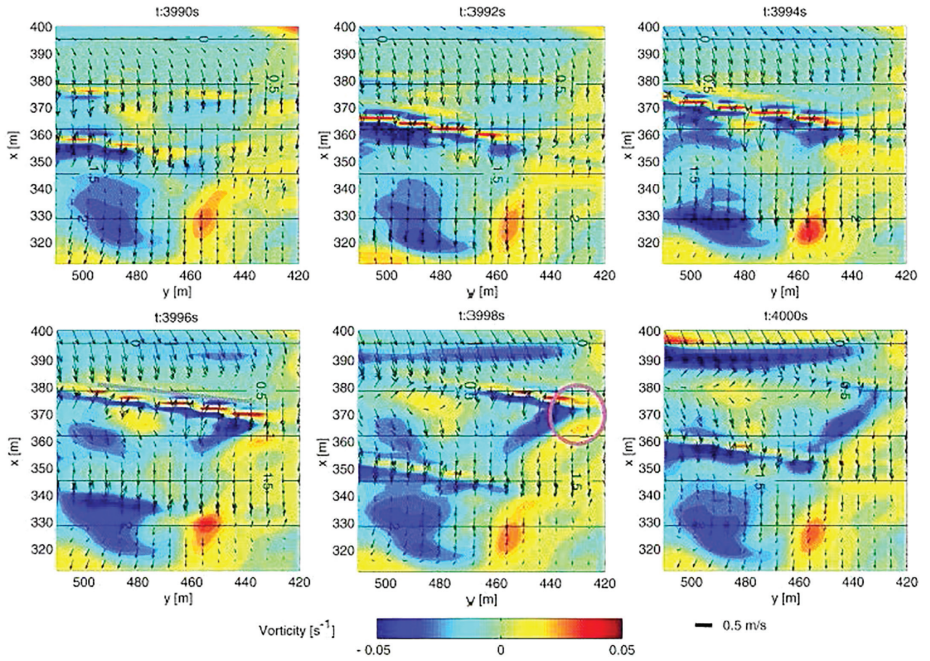

Figure 2. Generation of local vorticity patches at ends of breaking wave crests. (Reprinted from Johnson and Pattiaratchi (2006) with permission from Elsevier).

forcing, and a wave-averaged circulation model forced smoothly by radiation stress gradients derived from the incident wave conditions. Both studies showed the presence of a strongly energetic flow field in frequency and alongshore wavenumber space lying along a line that represents the local mean alongshore current velocity, representing the alongshore transport of eddy structures by the mean current. Feddersen showed that the wave-averaged model, with a spatially smooth wave forcing consistent with the statistical averaging of the wave field, did not generate a comparably energetic flow field particularly at higher frequencies and wavenumbers (Fig. 3).

Figure 4 shows a more detailed simulation of a localized wave-breaking event carried out using the LES/VOF model of Derakhti and Kirby (2014). The flow field is characterized by a large vortex loop that spans the entire breaking event, in a manner consistent with the generation mechanism of Peregrine (1998) as elaborated for deeper-water breaking by Pizzo and Melville (2013). The vortex loop retains a very highly concentrated, intense core, however, similar in form to the smaller-scale horseshoe vortices evolving in the confined region of active breaking. The larger scale loop elongates as it is left behind by the propagating crest, forming more oblique eddies that interact with the bottom in a complex fashion. This behavior persists for the entire range of breaking events from intermediate to shallow

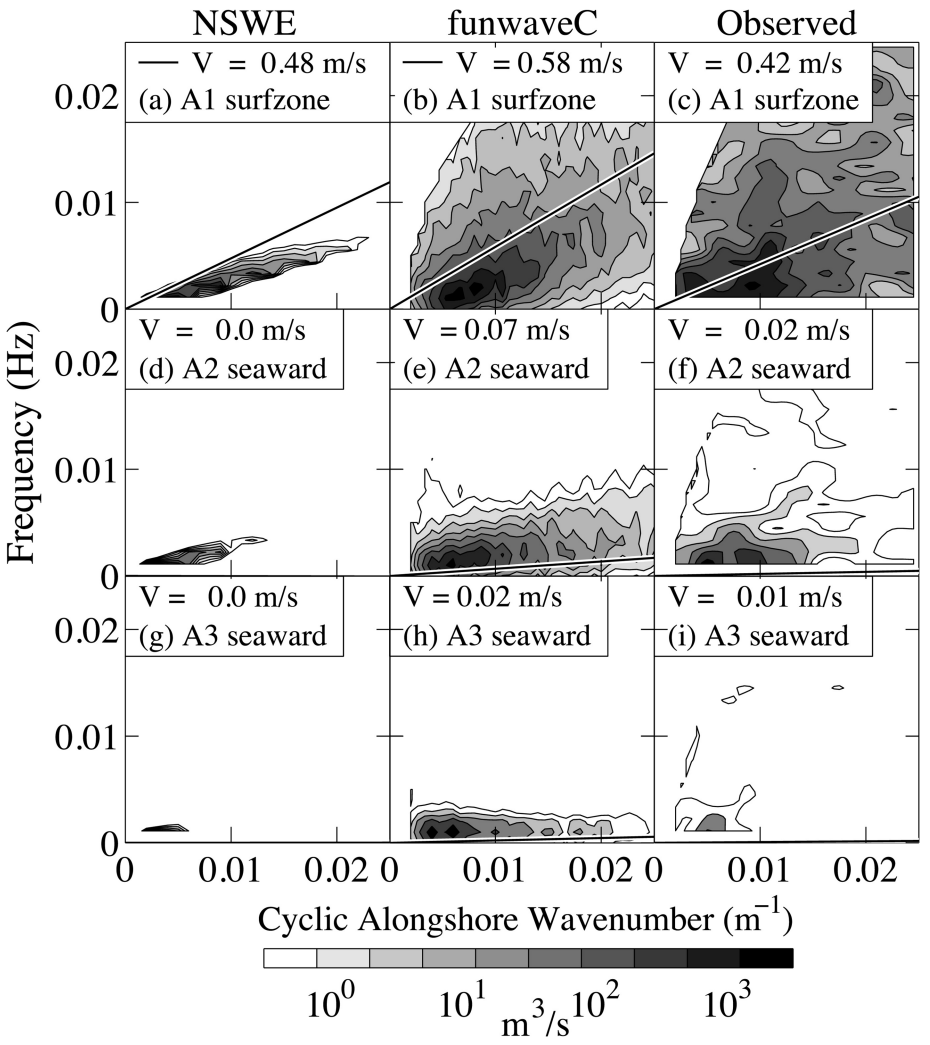

Figure 3. SandyDuck experiment (0828) cross-shore velocity alongshore wavenumber frequency spectra $E(f, k_y)$ for (left) wave-averaged model, (center) wave-resolving model, and (right) observations at cross-shore locations (top) in surf zone, (middle) just seaward of surf zone, and (bottom) well seaward of surf zone. V is the local mean alongshore, wave-averaged current. (Reprinted from Feddersen (2014); ©American Meteorological Society. Used with permission).

water, and implies the existence of a complex 3D structure of vortices and turbulence under individual short-crested breakers. The relationship between this complex pattern and the resultant depth-integrated pattern of vertical vorticity described by Peregrine (1998) and verified in depth-integrated model simulations (Johnson and Pattiaratchi 2006; Feddersen 2014; Choi et al. 2015) remains to be examined in detail.

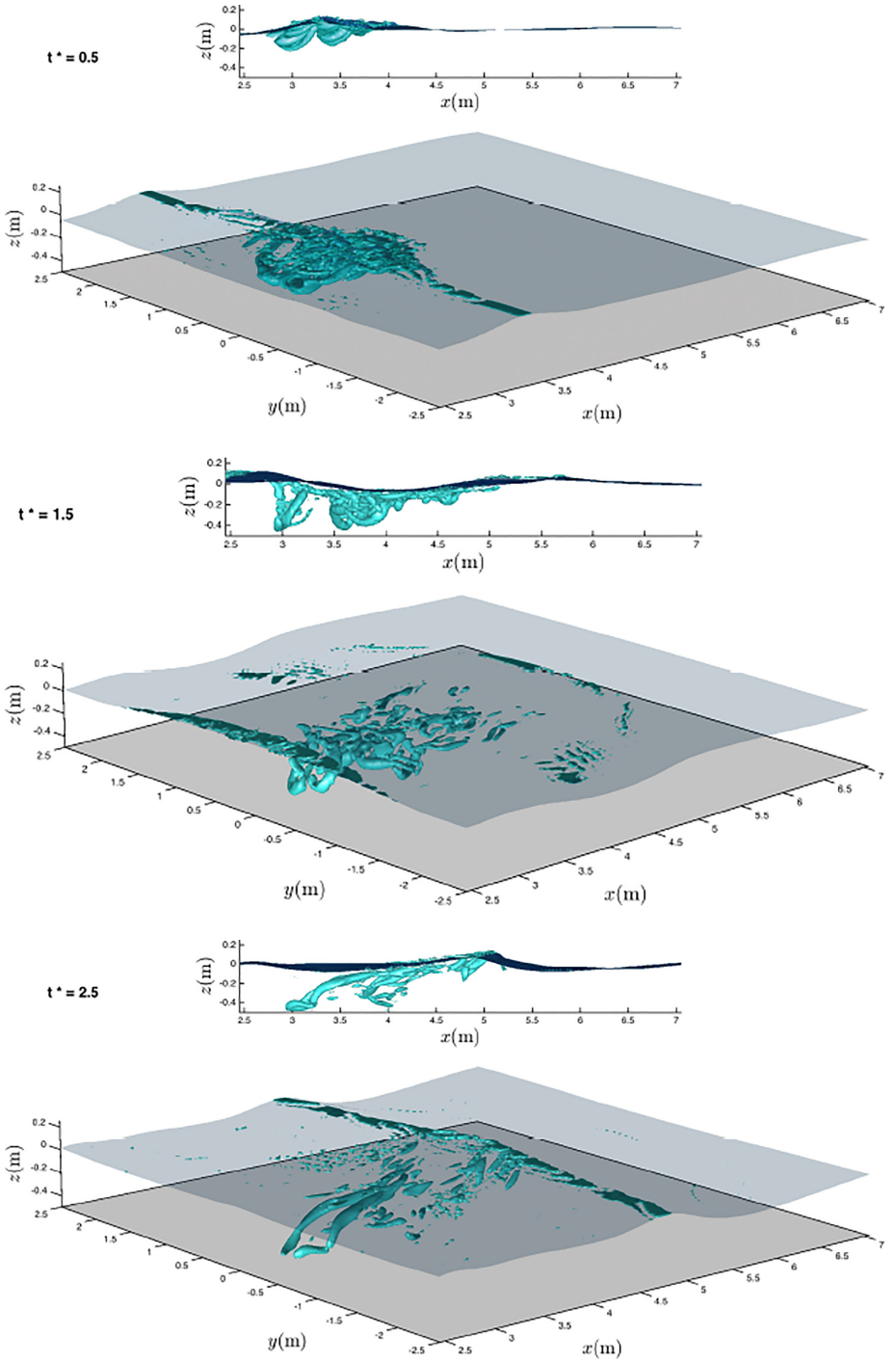

Figure 4. Snapshots of water surface and coherent structures for an isolated, short-crested breaking event. An initial, horseshoe-like vortex filament spanning the width of the breaker is generated, then elongates and moves downward until it interacts with the bottom.

b. Wave breaking over steep reefs

Breaking of groupy wave trains can generate strong, low-frequency waves (or "surf beat") in the surf zone through a combination of local forcing and release of bound incident waves (see (Baldock 2006) and references therein). Recently, it has become clear that the shoreward progressive components of such waves can steepen to the point of breaking, forming bore fronts that are comparable in magnitude to the incident wind waves and that represent rapidly varying transitions at the onset of strong onshore flows associated with the group frequencies (Van Dongeren et al. 2007). Bore formation is favored over low bottom slopes, where the shoaling long wave has time to steepen and break. Recently, this phenomenon has drawn attention as part of the study of wave breaking and induced currents over reefs, where strong breaking effects are localized at the seaward reef crest, after which the flat reef platform provides the low slope environment, allowing the low-frequency wave to steepen. The resulting bore fronts are thought to contribute to the rapidly varied flow conditions noted, for example, during Typhoon Haiyan in the Philippines, where strong surges with bore-like behavior were noted in flooded areas that were far beyond the reach of incident wind waves or well, which are largely dissipated at the reef margin (Roeber and Bricker 2015). Using a Boussinesq model, Nwogu and Demirbilek (2010) studied this phenomenon experimentally and numerically, and clearly showed that motions on the reef platform were dominated by waves in the frequency band associated with the incident wave group structure. They concluded that the principal response of the reef platform occurred at the first normal mode frequency for oscillation of water over the reef platform. Roeber and Bricker (2015) performed similar numerical experiments using 1D bathymetric profiles, which were chosen to be consistent with the region near Hernani, Philippines, which was impacted by Typhoon Haiyan. Their results also confirm the rapid decay of incident waves and the release and eventual steepening and breaking of infragravity waves propagating over the reef platform. They also showed that the observed strong motions did not occur at estimated normal mode frequencies for the reef and concluded that resonance is not required to obtain the strong response to wave group forcing, although they speculate that resonances could possibly worsen the already dangerous intensity of the low-frequency motions.

7. Transport and horizontal mixing processes

The generation of vertical vorticity at the scale of individual breaking wave crests, and the subsequent inverse cascade towards transient, large-scale eddies and rip currents, provides a mechanism for mixing of the surf zone volume and for exchange of water and materials between the surf zone and inner shelf regions. This mechanism is energetic and likely dominates over larger-scale mechanisms such as tidal and wind-driven currents and Stokes transport, which are more dominant at the scale of the shelf. This situation, again, points to the need for the additional information on wave breaking provided by Boussinesq or nonhydrostatic models when considering the region close to shore.

a. Surf zone horizontal mixing

Numerical experiments on mixing and transport processes associated with the generation of vorticity by short crested waves were carried out by Spydell and Feddersen (2009). They considered normally incident, directionally spread waves and concentrated on the evaluation of Lagrangian particle statistics and the estimation of surf zone diffusivity. Similar studies were carried out by Feddersen et al. (2011) and Clark et al. (2011) for obliquely incident waves, where the resulting mean-flow shear of the alongshore current contributes a Taylor dispersion-like component to the overall dispersion process (Smith 1995). All of these studies, in that waves are propagating and breaking over alongshore uniform bathymetry, show flow complexity and mixing processes in wave-resolved calculations that are consistent with observations and much stronger than predicted by wave-averaged models, with dispersion dominated by rotational eddies (Spydell and Feddersen 2009). (Indeed, in the case of normally incident waves (Johnson and Pattiaratchi 2006; Spydell and Feddersen 2009), a wave-averaged model would simply predict setup with no resulting mean flow.) The transient rip currents observed in these flows are essentially a consequence of the structure of a two-dimensional turbulent flow, with inverse cascading of wave-induced, small-scale vorticity to larger-scale eddies that are manifested as rips.

In contrast, Geiman et al. (2011) carried out a similar model/model/data comparison for waves incident over a complex beach incised by rip channels located reasonably regularly in the alongshore direction. Lagrangian particle trajectories were computed using model-generated flow fields from wave-averaged and wave-resolving models and then used to compute particle separation statistics, a precursor to deriving diffusion estimates. Model-generated statistics were compared to each other and to similar statistics derived from drifter trajectories in the field. Results indicated that apparent diffusivity is basically the same for the wave-averaged and wave-resolving models, with both in general agreement with field observations. Clearly, conditions here are very different from the case of waves incident on a featureless beach, where the spatial scale associated with the short-crestedness of waves is the only scale imposed on the problem. For the case with rip channels, the channels appear to provide the dominant scale, with differences between smooth and irregular wave forcing lost in the noise. These results are distinct, and point to some middle ground where controlling scales supplied by different mechanisms are comparable in importance and can interact in a more balanced way, with unforeseeable outcome.

Very few BTM models address the presence of turbulence and vorticity in a direct manner. All BTM models with advective acceleration effects in the horizontal flow field can advect vertical vorticity once it is generated, but do not address horizontal vorticity associated with turbulent velocity profiles or interaction between the components. Lateral mixing effects resulting from turbulence are often handled using Smagorinsky-like diffusion operators, as is common in ocean modeling, and bottom friction is treated using standard quadratic formulations based on depth-averaged velocity with calibrated friction coefficients. Kim et al. (2009) have developed a more comprehensive treatment of the depth-averaged flow field, taking into account the presence of turbulence and vorticity. Kim and Lynett (2011)

further developed a depth-integrated scalar transport equation along similar lines. Kim (2015) used this model together with an erosion/deposition model to simulate suspended sediment flux and resulting morphology adjustment. Kim and Lynett (2013) instead used a σ coordinate transport model in 3D, with the upper boundary determined by the BTM. This configuration becomes more like a 3D NHM formulation (Ma et al. 2013a) but with the velocity field determined semi-analytically from the depth-integrated BTM. This sequence of papers represents a concerted effort to inject missing physics (turbulence, vorticity, and mixing) into the BTM framework, which is usually based on the inviscid Euler equations as a starting point, with additional effects added in an ad hoc fashion. The development is largely concentrated on representing vorticity induced by the bottom, through the choice of eddy viscosity distribution and boundary conditions. In contrast, Richard and Gavrilyuk (2013) describe a model where the presence of vorticity associated with breaking-induced (or, more properly, bore-induced) turbulence and shear plays a central role. This model has been further extended by Richard and Gavrilyuk (2015) to include solitary wave behavior, but it has not been generalized for application as a fully two-dimensional model for use over arbitrary bathymetry.

It has not been clearly demonstrated that the extra care taken to develop these extensions to the simpler BTM framework (i.e., of a flow with no horizontal vorticity and extra physical effects added in an ad-hoc manner) produces an obviously superior model in terms of predictive capabilities. The studies of Spydell and Feddersen (2009) and Clark et al. (2011) show satisfactory agreement in predictions of surf zone diffusivities when compared to observations, and similar skill levels are obtained for basic wave processes (Feddersen 2014; Choi et al. 2015) using models based on the limited physics of Euler equations. The need for the extended physics of these models within the context of the depth-integrated Boussinesq framework continues to be assessed.

b. Surf zone - inner shelf exchange

In the inner to mid-shelf region, outside of the dissipation-dominated surf zone, wave-averaged models have been shown to provide an accurate description of wind and tidally driven processes at semidiurnal and diurnal (Kumar et al. 2016) and subtidal (Kumar et al. 2015) time scales. Models such as ROMS are skillful predictors of processes such as fresh-water plume dispersion from small streams (Romero et al. 2016).

At smaller scales, the energetic mixing caused by complex patterns of wave breaking can dominate the problem. Suanda and Feddersen (2015) recently considered the implications of the development of transient rip currents in normally incident, directionally spread waves (Johnson and Pattiaratchi 2006; Spydell and Feddersen 2009) on possible exchange of material between the surf zone and inner shelf. Suanda and Feddersen established a self-similar scaling for cross-shore exchange velocity (based on alongshore averages of rotational cross-shore velocity components in simulated flow fields) as a function of cross-shore distance normalized by surf zone width. They found that a time scale for surf zone flushing is inversely proportional to the directional spread of incident waves, with more directionally

spread waves implying increased short-crested breaking, vorticity generation, and greater cross-shore mixing. On average, cross-shore exchange velocity resulting from transient eddy motions dominates over return flows associated with Stokes drift for up to two to six times the nominal surf zone width. It is worth reiterating that this efficient transport mechanism does not take place in a conventional wave-averaged model, where the effect of short-crested breaking waves is not considered. Hally-Rosendahl and Feddersen (2016) performed a similar study of exchange with the inner shelf in an energetic alongshore current. They concluded that this exchange was similar in mechanism to the exchange in shore-normal waves (with no mean alongshore current) and was a major component of the apparent dilution of dye concentration along shore, with up to 50% of total dye volume transferred to the inner shelf by mixing.

c. Lagrangian coherent structures as a diagnostic tool

Model simulations of nearshore current patterns provide the potential for a more complete understanding of transport and mixing patterns than is available from drifter trajectories, whether measured or synthetic. In particular, model results provide information for regions that are denied to a potential drifter population due to flow related transport barriers. Following on earlier work at continental shelf scale, Reniers et al. (2010) employed a dynamical systems approach known as Lagrangian Coherent Structure (LCS) analysis (Haller 2000), to examine the mechanisms for the observed tendency for rip currents on a beach with extensively incised rip channels to retain drifters in the dominant rip-current circulation pattern rather than ejecting them offshore (Reniers et al. 2009). Their results showed a correspondence between episodes of drifter ejection and the detachment of eddies from the main rip current circulation pattern associated with very low-frequency surf zone oscillations. The importance of this analysis tool for studies of swimmer safety and transport of pollutants, larvae, and pathogens has been further explored in additional studies (Fiorentino et al. 2012, 2014), and the technique should see more utilization in the future. All of these studies and conclusions are based on the use of wave-averaged models, and it is not known how wave-resolving computations would possibly alter overall flow structures or diffuse the identity of manifolds (or boundaries between dynamically separated regions).

8. Waves on sheared mean currents

Waves in coastal settings may encounter strong currents that are sheared in the vertical, either through the effects of bottom stress and turbulence, or in response to inhomogeneities such as density stratification. The theory of either wave-averaged or wave-resolving models does not usually encompass this case, where vorticity may be strong and three-dimensional. Earlier studies by Stewart and Joy (1974), Skop (1987), Kirby and Chen (1989) have provided a perturbation approach and lowest-order results for the description of waves on weak currents of arbitrary vertical distribution. ("Weak currents" denotes a regime where the ratio of current speed/wave phase speed is small, and leads to the irrotational solution for waves

propagating relative to a stationary water column as the leading term.) Ardhuin et al. (2008) and others have suggested using the depth-weighted current speed (Skop 1987; Kirby and Chen 1989)

$$\tilde{U} = \frac{2kh}{\sinh 2kh} \int_{-h}^{0} U(z) \cosh 2h(h+z) dz \tag{15}$$

which appears in the theory as the leading order phase speed correction due to the presence of a depth-varying current, as a choice for the current velocity in the wave action balance equation that is central to all spectral wave models. This approach has been incorporated as an option in several popular ocean circulation models including Delft 3D (Elias et al. 2012) and ROMS/COAWST (Warner et al. 2010). Banihashemi et al. (2017) point out that the approach used to date is problematic for several reasons. First, as originally indicated by Kirby and Chen (1989), $\tilde{U}$ is not the apparent current speed in the expression for group velocity; differentiation of the dispersion relation $\omega = \sigma + k\tilde{U}$ w/r k (where ω is wave frequency in a stationary frame and σ is the intrinsic wave frequency relative to a frame moving with the current) gives

$$\hat{U} = \tilde{U} + k\frac{\partial \tilde{U}}{\partial k} \tag{16}$$

as the most logical choice for the current advection velocity for wave action. Banihashemi et al. (2017) affirm this conclusion and examine the errors involved in using $\tilde{U}$ rather than $\hat{U}$, which can become quite large in extreme conditions such as those occurring during ebb-tidal conditions in the mouth of the Columbia River (Kilcher and Nash 2010; Elias et al. 2012). Figure 5 shows a plot of the difference between absolute and relative group velocities C_{ga} and C_{g0} normalized by $\tilde{U}$ (15) for the case of a current with constant shear given by

$$U(z) = U_s \left(1 + \alpha \frac{z}{h}\right) \tag{17}$$

Results are shown for the first two corrections in the perturbation solution, where frequency and group velocity are given by

$$\omega = \sigma_0 + (F)\sigma_1 + (F^2)\sigma_2 = \sigma_0 + k\tilde{U} + kC_2 \tag{18}$$

$$C_{ga} = \frac{\partial \sigma_0}{\partial k} + (F)\frac{\partial \sigma_1}{\partial k} + (F^2)\frac{\partial \sigma_2}{\partial k} = C_{g0} + \hat{U} + \frac{\partial \sigma_2}{\partial k} \tag{19}$$

with

$$\sigma_0^2 = gk \tanh kh \tag{20}$$

and where $F = U_s/\sqrt{gh}$ representing a Froude number based on the current speed at the surface, with ordering in F indicated schematically. The range $0 \leq \alpha \leq 1$ corresponds to

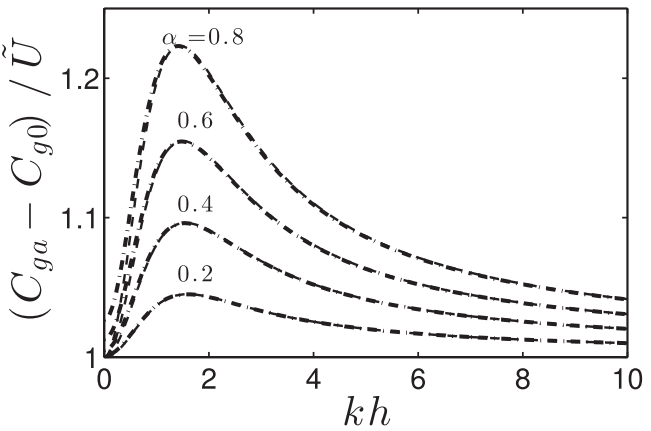

Figure 5. Correction to group velocity $(C_{ga} - C_{g0})/\tilde{U}$ vs relative depth kh for various choices of constant vertical current shear $\alpha U_s/h$. Dashed lines: $O(F)$ approximation. Solid lines: $O(F^2)$ approximation.

currents with velocity at the bottom varying from U_s (the depth-uniform case) to 0. The error in using $\tilde{U}$ in place of $\hat{U}$ can become significant, and is even more problematic for strongly sheared currents resulting during formation of buoyant ebb-tidal surface plumes. In contrast, the gain associated with using the estimate for current speed to $O(F^2)$ is generally minor and is most likely not needed for practical use. Further, the use of a single current speed rather than a frequency-dependent, depth-weighted speed in SWAN, the model most commonly coupled to nearshore-ocean circulation models, also entails a rapid accumulation of error in current speed estimates away from the usual reference point of peak frequency. These limitations need to be actively explored as part of ongoing model development.

For the case of depth-integrated BTMs, two early treatments of the problem are the works of Rego et al. (2001), who used an approach which was limited to one horizontal dimension and used a scalar stream function to represent the rotational part of the wave and current field, and Shen (2001), who provided a different formulation based on the vertical velocity w as the main dependent variable, which is a natural choice in developing wave-current models as it generalizes the stream function problem to three dimensions in a straightforward way (McWilliams et al. 2004). Both derivations only treat the inviscid Euler equations, and thus details about the vorticity distribution have to be imposed externally, either directly (Shen 2001), or through specification of a mean current profile (Rego et al. 2001). More recently, Son and Lynett (2014) have generalized the rotational Boussinesq model of Kim et al. (2009) to include the presence of a sheared, turbulent mean flow.

All of these treatments depend on the specification of a current field, which waves then interact with. This implies that, in a realistic setting, one would need to run a circulation model to provide the current, and then a Boussinesq model with circulation model results

provided as input. The Boussinesq model results could, in principle, be used to develop wave forcing for the circulation model, and the two could be run in a fully coupled fashion. The newly available nonhydrostatic models largely eliminate this necessity by providing a unified simulation of the entire flow field at resolutions comparable to usual choices for the Boussinesq model.

9. Sediment transport and morphology change

Nearshore hydrodynamic models provide the crucial forcing input for models of coastal morphology evolution. Models of morphology change have evolved rapidly, in parallel with the maturation of ocean circulation models. This subject is itself vast, involving modeling of scales from grain diameter to decades or centuries of morphology evolution. A comprehensive introduction to the present state of modeling approaches may be found in Roelvink and Reniers (2012).

Morphology evolution involves an interplay between the grain and bedform-scale process modeling of the sediment entrainment, transport and deposition, variations of these processes with changing wave and current conditions at surf zone or nearshore scale, and self-organizational principles acting at the scale of largest planform features such as cuspate shorelines and bar configurations. For the most part, notions about the construction of sediment transport formulas have evolved slowly over time. Recently introduced concepts include the consideration of free stream velocity skewness and asymmetry and resulting effects on bed stress due to phase shifts across the wave boundary layer (Nielsen and Callaghan 2003) and the notion that strong horizontal fluid accelerations (or, equivalently, pressure gradients) can lead to bulk destabilization of the sediment bed, resulting in "plug flow" (Sleath 1999; Foster et al. 2006). The role of acceleration in transport of course particles is also considered by Drake and Calantoni (2001). Improvements in understanding of the local processes affecting transport rate will certainly continue with improved instrumentation and direct measurement of near-bed stress and velocities at the granular level.

At the opposite extreme, considerations of large-scale organization have played an important role in the development of the topic. Concentrating, for example, on the historical development of cross-shore profile models, this approach has continued and expanded to include studies of the persistence and interaction of shore-parallel bars. Ruessink et al. (2007) and Ruessink and Kuriyama (2008) employed a process-based model to examine factors controlling onshore or offshore bar migration. Predicting the behavior of the inner, or most landward, bar on a multi-bar profile proved difficult, and drops in model skill level relative to observations were most often associated with significant alongshore variations in planform. Using a 2D, depth-integrated morphology model, Smit et al. (2012) considered the effect of morphological variability on planform evolution. They concluded that deeply imprinted morphology patterns such as established crescentic bars are much less susceptible to rapid change than are beaches without significant alongshore variability. Planform

studies reveal difficulties in conceptual behavior of 1D cross-shore models; for example, Walstra et al. (2015) have reported the inability of a 1D model to describe discontinuous patterns of offshore bar migration known as "bar switches," which are necessarily related to bar morphologies, which are discontinuous in the alongshore direction and thus likely affected by 3D circulation patterns.

As experience with large-scale process models grows, models continue to be applied to a wider range of settings including open coasts and offshore bars, inter-tidal sand banks and tidal flats, estuarine and riverine environments, and tidal wetlands. Improvements in model performance and predictability are likely to continue, leading to models with potential for predictive capabilities over long time scales, given reliable estimates of wave climatology and the resources needed to carry out large ensembles of simulations.

a. Acceleration techniques

Time-scales for morphology adjustment are typically long compared to the hydrodynamic time scales associated with tides or inhomogeneities in wave conditions, the exceptions being extreme cases such as tsunamis or intense storms. The development of an understanding of coastal morphology evolution depends on an accurate prediction of tides and the statistics of wave climate and storm occurrence. The need to carry such predictions out for decadal or longer time scales imposes a heavy burden on the hydrodynamic calculation, where time steps are limited by Froude number criteria and are small in comparison to the hydrodynamic time scales. Various strategies have thus been developed in order to estimate the incremental, long-time sedimentary response to the range of instantaneous conditions seen in the hydrodynamics. The most favored approach in use today involves the specification of a "morphology factor" n, which multiplies the rate of depth change computed during a resolved model time step. Early versions of this approach involved computing the net change of bed elevation over a tide cycle, and then multiplying the change by the number of tide cycles of similar form during the simulation period. This process could be carried out for a set of representative tide cycles, leading to a prediction of morphology change for the period of interest. The approach is often unstable, and has not seen widespread adoption.

A different approach has been developed by Roelvink (2006). As an alternate to tidal-averaging, bed level changes can be computed instantaneously during the hydrodynamic calculations and then multiplied by the morphology factor. Running the model for one tide cycle then amounts to evolving the bed for n tide cycles, the difference from the previous approach being that the hydrodynamics and morphology calculations both experience the bed change during the simulated cycle. Roelvink (2006) showed that the stability of this approach is improved by running several simulations in parallel with staggered start times but a continual application of inter-model corrections to bathymetry changes which serve to average out anomalous features occurring in any member of the ensemble. Shi et al. (2015a) discuss additional modifications to the approach to account for artificial changes arising from an initial imbalance between the assumed planform and the planform that would be in equilibrium with the initial wave conditions.

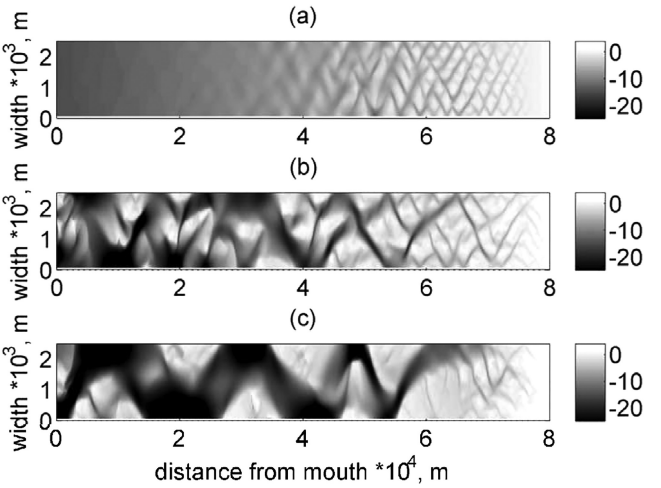

Figure 6. Pattern formation for the shallow basin in meters (2.5 km wide and 80 km long), (a) after 15 years, (b) after 100 years, (c) after 800 years. Not to scale. (Reprinted from van der Wegen and Roelvink (2008)).

The morphology factor has proven to be a powerful concept in coastal morphology modeling, with simulations of coastal planform response to tidal forcing now extending to centuries (van der Wegen and Roelvink 2008; van der Wegen et al. 2008), as illustrated in Figure 6.

10. Discussion

The capability of both 2D and 3D wave-resolving models to reproduce surf zone dynamics down to scales of breaking wave crests is currently well developed, although more work remains to be done to understand details of transport pathways at this scale. Further extension of 2D BTM models to include information about sediment load or stratification and resulting baroclinic motion implies the use of an additional 3D model, which may in turn be fully coupled and driven with averaged results from the BTM model. This complexity is circumvented completely by using fully 3D nonhydrostatic models, which can resolve wave motion at the same resolution as the depth-integrated 2D models, and which are easily extended to incorporate additional physical effects. The nonhydrostatic model thus appears to be a clear and natural choice for use in problems where information about wave geometry and 3D structure of fields such as temperature or salinity are needed.

The lack of a localized forcing mechanism corresponding to short-crested breaking in typical wave-averaged model formulations is a drawback that hinders proper model prediction of the magnitude and scale of vorticity generation and its impact on circulation and mixing. This problem has been handled adequately in deep water using stochastic

formulations, which only need to reproduce the strength and probability of occurrence of uniformly distributed whitecap events to provide a proper representation of episodic vorticity injection and impact on the upper ocean mixed layer. Extraction of the vorticity-forcing fields can, in principle, be derived from a BTM model run in parallel and injected into the wave-averaged model, but this would again point to the advantages of simply running a nonhydrostatic model for the entire flow field instead. Development of a methodology for specifying this forcing based only on the circulation model and coupled spectral wave model would be a major benefit to the further development of surf zone models.

The problem of prediction for the nearshore region is complicated by a number of factors. First, there is the physical scale of the problem. Models for surf zone dynamics can require model resolutions on the order of meters, and thus a detailed model of several kilometers of coastline can approach in size a model for hundreds of kilometers of adjacent shelf regions. Detailed modeling of nearshore regions is thus usually approached in a research context and is often tied to short-term field measurement programs. The resources for carrying out continued, detailed modeling of a wide selection of nearshore regions does not really exist. Secondly, correct forcing of nearshore models depends on an accurate prediction of tidal currents, wind fields, and wave conditions. Models for tidal motion, subtidal motion, and wind fields are becoming more readily available. They can provide needed input for nearshore models, and they are now frequently run in forecast model for large areas at relatively low resolution. Progress is being made in providing forecasts of wave conditions in conjunction with general weather predictions. For example, the National Centers for Environmental Modeling (National Weather Service (NWS), NOAA) now provide predictions of global wave conditions extending out 180 hours, with predictions updated four times a day (http://polar.ncep.noaa.gov/). More recently, global predictions of this sort are augmented by more detailed wave modeling using models such as SWAN (Booij et al. 1999), forced by global model results offshore and by real-time predictions of wind and current fields. An analysis of model skill for the NWS Nearshore Wave Prediction System may be seen at (http://polar.ncep.noaa.gov/nwps/). Modeling of this sort is expected to be most accurate in regions dominated by wind seas generated at short to moderate fetches. Crosby et al. (2016) describe an effort to augment such a prediction capability by accounting for swell conditions, representing longer period dispersed wave trains that are not handled well by most spectral wave models. Using ray methods to transform swell energy in the 0.04–0.09 Hz range, Crosby et al. (2016) show an improved capability to predict wave conditions inshore in a complex coastal region in comparison to purely spectral model results, but show that a great deal of uncertainty in predictions of nearshore processes is still associated with the process of specifying offshore boundary conditions. Thus, it is clear that the process of predicting nearshore physical processes will be hampered for some time by inaccuracies in predicting forcing conditions using readily available products, aside from any remaining limitations in the nearshore modeling capabilities themselves.

Acknowledgments. I would like to thank the Office of Naval Research, the Army Research Office, the National Science Foundation, and the Delaware Sea Grant Program for their support over the years. This work was funded by NSF grants OCE-1334325, OCE-1435147, CMMI-1537232 and by the National Tsunami Hazard Mitigation Program. Figure 4 was provided by Morteza Derakhti. I would like to thank Falk Feddersen and a second reviewer for their constructive comments on the original manuscript.

REFERENCES

Allen, J. S., P. A. Newberger, and R. A. Holman. 1996. Nonlinear shear instabilities of alongshore currents on plane beaches. J. Fluid Mech., *310*, 181–213. doi: 10.1017/S0022112096001772

Apotsos, A., B. Raubenheimer, S. Elgar, and R. T. Guza. 2008. Testing and calibrating parametric wave transformation models on natural beaches. Coast. Eng., *55*, 224–235. doi: 10.1016/j.coastaleng.2007.10.002

Ardhuin, F., N. Rascle, and K. A. Belibassakis. 2008. Explicit wave-averaged primitive equations using a generalized Lagrangian mean. Ocean Model., *20*, 35–60. doi: 10.1016/j.ocemod.2007.07.001

Baldock, T. E. 2006. Long wave generation by the shoaling and breaking of transient wave groups on a beach. Proc. R. Soc. A, *462*(2070), 1853–1876. doi: 10.1098/rspa.2005.1642

Banihashemi, S., J. T. Kirby, and Z. Dong. 2017. Approximation of wave action flux velocity in strongly sheared mean flows. Ocean Model., *116*, 33–47, doi: 10.1016/j.ocemod.2017.06.002

Battjes, J. A., and J. P. F. M. Janssen. 1978. Energy loss and setup due to breaking of random waves. In *Proc. 16th Conference on Coastal Engineering*, Hamburg, Germany, 1978 (ASCE; American Society of Civil Engineers), *16*, 569–587. doi: uuid:2fba43fe-f8bd-42ac-85ee-848312d2e27e

Bonneton, P., E. Barthelemy, F. Chazel, R. Cienfuegos, D. Lannes, F. Marche, et al. 2011a. Recent advances in Serre-Green Naghdi modelling for wave transformation, breaking and runup processes. Eur. J. Mech. B-Fluid, *30*, 589–597. doi: 10.1016/j.euromechflu.2011.02.005

Bonneton, P., F. Chazel, D. Lannes, F. Marche, and M. Tissier. 2011b. A splitting approach for the fully nonlinear and weakly dispersive Green-Naghdi model. J. Comput. Phys., *230*, 1479–1498. doi: 10.1016/j.jcp.2010.11.015

Booij, N., R. C. Ris, and L. H. Holthuijsen. 1999. A third-generation wave model for coastal regions: 1. Model description and validation. J. Geophys. Res. Oceans, *104*(C4), 7649–7666. doi: 10.1029/98JC02622

Boussinesq, J. 1872. Théorie des ondes et des remous qui se propagent le long d'un canal rectangulaire horizontal, en communiquant au liquide contenu dans ce canal des vitesses sensiblement pareilles de la surface au fond. J. Math. Pures Appl. (Series 2), *17*, 55–108.

Bowen, A. J. 1969a. Rip currents: 1. Theoretical investigations. J. Geophys. Res. Oceans Atmos., *74*(23), 5467–5478. doi: 10.1029/JC074i023p05467

Bowen, A. J. 1969b. The generation of longshore currents on a plane beach. J. Mar. Res., *27*, 206–215.

Bowen, A. J., D. L. Inman, and V. P. Simmons. 1968. Wave 'set-down' and set-up. J. Geophys. Res. Oceans Atmos., *73*(8), 2569–2577. doi: 10.1029/JB073i008p02569

Bradford, S. F. 2005. Godunov-based model for nonhydrostatic wave dynamics. J. Waterw. Port Coast. Ocean Eng., *131*(5), 226–238. doi: 10.1061/(ASCE)0733-950X(2005)131:5(226)

Bradford, S. F. 2011. Nonhydrostatic model for surf zone simulation. J. Waterw. Port Coast. Ocean Eng., *137*(4), 163–174. doi: 10.1061/(ASCE)WW.1943-5460.0000079

Bretherton, F. P., and C. J. R. Garrett. 1968. Wavetrains in inhomogeneous moving media. Proc. R. Soc. A, *302*(1471), 529–554. doi: 10.1098/rspa.1968.0034

Brocchini, M. 2013. A reasoned overview on Boussinesq-type models: the interplay between physics, mathematics and numerics. Proc. R. Soc. A, *469*(20130496). doi: 10.1098/rspa.2013.0496

Bühler, O., and T. E. Jacobson. 2001. Wave-driven currents and vortex dynamics on barred beaches. J. Fluid Mech., *449*, 313–339. doi: 10.1017/S0022112001006322

Casulli, V. 1999. A semi-implicit finite difference method for non-hydrostatic, free-surface flows. Int. J. Numer. Methods Fluids, *30*, 425–440. doi: 10.1002/(SICI)1097-0363(19990630)30:4<425::AID-FLD847>3.0.CO;2-D

Casulli, V., and G. S. Stelling. 1998. Numerical simulation of 3D quasi-hydrostatic, free surface flows. J. Hydraul. Eng.-ASCE, *124*(7), 678–686. doi: 10.1061/(ASCE)0733-9429(1998)124:7(678)

Chen, Q. 2006. Fully nonlinear Boussinesq-type equations for waves and currents over porous beds. J. Eng. Mech.-ASCE, *132*(2), 220–230. doi: 10.1061/(ASCE)0733-9399(2006)1232:2(220)

Chen, Q., R. A. Dalrymple, J. T. Kirby, A. B. Kennedy, and M. C. Haller. 1999. Boussinesq modeling of a rip current system. J. Geophys. Res. Oceans, *104*(C9), 20617–20637. doi: 10.1029/1999JC900154

Chen, Q., J. T. Kirby, R. A. Dalrymple, F. Shi, and E. B. Thornton. 2003. Boussinesq modeling of longshore currents. J. Geophys. Res. Oceans, *108*(C11), 3362. doi: 10.1029/2002JC001308

Choi, J., J. T. Kirby, and S. B. Yoon. 2015. Boussinesq modeling of longshore currents in the Sandy-Duck experiment under directional random wave conditions. Coast. Eng., *101*, 17–34. doi: 10.1016/j.coastaleng.2015.04.005

Cienfuegos, R., E. Barthélemy, and P. Bonneton. 2010. Wave-breaking model for Boussinesq-type equations including roller effects in the mass conservation equation. J. Waterw. Port Coast. Ocean Eng., *136*(1), 10–26. doi: 10.1061/(ASCE)WW.1943-5460.0000022

Clark, D. B., F. Feddersen, and R. T. Guza. 2011. Modeling surf zone tracer plumes: 2. Transport and dispersion. J. Geophys. Res. Oceans, *116*, C11028. doi: 10.1029/2011jc007211

Clark, D. B., S. Elgar, and B. Raubenheimer. 2012. Vorticity generation by short-crested wave breaking. Geophys. Res. Lett., *39*, L24604. doi: 10.1029/2012GL054034

Craik, A. D. D., and S. Leibovich. 1976. A rational model for Langmuir circulation. J. Fluid Mech., *73*(3), 401–426. doi: 10.1017/S0022112076001420

Crosby, S. C., W. C. O'Reilly, and R. T. Guza. 2016. Modeling long-period swell in southern California: practical boundary conditions from buoy observations and global wave model predictions. J. Atmos. Ocean. Technol., *33*, 1673–1690. doi: 10.1175/JTECH-D-16-0038.1

Dalrymple, R. A., and B. D. Rogers. 2006. Numerical modeling of water waves with the SPH method. Coast. Eng., *53*, 141–147. doi: 10.1016/j.coastaleng.2005.10.004

Dalrymple, R. A., J. H. MacMahan, A. J. H. M. Reniers, and V. Nelko. 2011. Rip currents. Annu. Rev. Fluid Mech., *43*, 551–581. doi: 10.1146/annurev-fluid-122109-160733

Derakhti, M., and J. T. Kirby. 2014. Bubble entrainment and liquid bubble interaction under unsteady breaking waves. J. Fluid Mech., *761*, 464–506. doi: 10.1017/jfm.2014.637

Dingemans, M. W., A. C. Radder, and H. J. De Vriend. 1987. Computation of the driving forces of wave-induced currents. Coast. Eng., *11*, 539–563. doi: 10.1016/0378-3839(87)90026-3

Divoky, D., B. Le Méhauté, and A. Lin. 1970. Breaking waves on gentle slopes. J. Geophys. Res. Oceans Atmos., *75*(9), 1681–1692.

Drake, T. G., and J. Calantoni. 2001. Discrete particle model for sheet flow sediment transport in the neashore. J. Geophys. Res. Oceans, *106*(C9), 19859–19868. doi: 10.1029/2000JC000611

Elder, J. W. 1959. The dispersion of marked fluid in turbulent shear flow. J. Fluid Mech., *5*, 544–560. doi: 10.1017/S0022112059000374

Elias, E. P., G. Gelfenbaum, and A. J. Van der Westhuysen. 2012. Validation of a coupled wave-flow model in a high-energy setting: The mouth of the columbia river. J. Geophys. Res. Oceans, *117*(C09011). doi: 10.1029/2012JC008105

Farahani, R. J., and R. A. Dalrymple. 2014. Three-dimensional reversed horseshoe vortex structures under broken solitary waves. Coast. Eng., *91*, 261–279. doi: 10.1016/j.coastaleng.2014.06.006

Feddersen, F. 2014. The generation of surfzone eddies in a strong alongshore current. J. Phys. Oceanogr., *44*, 600–617. doi: 10.1175/JPO-D-13-051.1

Feddersen, F., D. B. Clark, and R. T. Guza. 2011. Modeling surf zone tracer plumes: 1. Waves, mean currents, and low-frequency eddies. J. Geophys. Res. Oceans, *116*, C11027. doi: 10.1029/2011jc007210

Fiorentino, L. A., M. J. Olascoaga, A. Reniers, Z. Feng, F. J. Beron-Vera, and J. H. MacMahan. 2012. Using Lagrangian Coherent Structures to understand coastal water quality. Cont. Shelf Res., *47*, 145–149. doi: 10.1016/j.csr.2012.07.009

Fiorentino, L. A., M. J. Olascoaga, and A. Reniers. 2014. Analysis of water quality and circulation of four recreational Miami beaches through the use of Lagrangian Coherent Structures. Mar. Pollut. Bull., *83*, 181–189. doi: 10.1016/j.marpolbul.2014.03.054

Foster, D. L., A. J. Bowen, R. A. Holman, and P. Natoo. 2006. Field evidence of pressure gradient induced incipient motion. J. Geophys. Res. Oceans, *111*, C05004. doi: 10.1019/2004JC002863

Geiman, J. D., J. T. Kirby, A. J. H. M. Reniers, and J. H. MacMahan. 2011. Effects of wave averaging on estimates of fluid mixing in the surf zone. J. Geophys. Res. Oceans, *116*, C04006. doi: 10.1029/2010JC006678

Gobbi, M. F., J. T. Kirby, and G. Wei. 2000. A fully nonlinear Boussinesq model for surface waves. Part 2. Extension to $O(kh)^4$. J. Fluid Mech., *405*, 181–210. doi: 10.1017/S0022112099007247

Green, A. E., and P. M. Naghdi. 1976. A derivation of equations for wave propagation in water of variable depth. J. Fluid Mech., *78*(2), 237–246. doi: 10.1017/S0022112076002425

Haas, K. A., and J. C. Warner. 2009. Comparing a quasi-3D to a full 3D nearshore circulation model: SHORECIRC and ROMS. Ocean Model., *26*, 91–103. doi: 10.1016/j.ocemod.2008.09.003

Haas, K. A., I. A. Svendsen, M. C. Haller, and Q. Zhao. 2003. Quasi-three-dimensional modeling of rip current systems. J. Geophys. Res. Oceans, *108*(C7), 3217. doi: 10.1029/2002JC001355

Haller, G. 2000. Finding finite-time invariant manifolds in two-dimensional velocity fields. Chaos, *10*, 99–108. doi: 10.1063/1.166479

Hally-Rosendahl, K., and F. Feddersen. 2016. Modeling surfzone to inner-shelf tracer exchange. J. Geophys. Res. *121*, 2007–2025. doi: 10.1002/2015JC011530

Hunt, J. C. R., A. A. Wary, and P. Moin. 1988. Eddies, streams and convergence zones in turbulent flows. Technical Report CTR-S88, *1*, 193–208, Stanford, CA: Center for Turbulence Research.

Ismail, N. M., and R. L. Wiegel. 1983. Opposing wave effect on the momentum jets spreading rate. J. Waterw. Port Coast. Ocean Eng., *109*(4), 465–483. doi: 10.1061/(ASCE)0733-950X(1983)109:4(465)

Johnson, D., and C. Pattiaratchi. 2006. Boussinesq modelling of transient rip currents. Coast. Eng., *53*, 419–439. doi: 10.1016/j.coastaleng.2005.11.005

Karambas, T. V., and C. Koutitas. 2002. Surf and swash zone morphology evolution induced by nonlinear waves. J. Waterw. Port Coast. Ocean Eng., *128*, 102–113. doi: 10.1061/(ASCE) 0733-950X(2002)128:3(102)

Kennedy, A. B., Q. Chen, J. T. Kirby, and R. A. Dalrymple. 2000. Boussinesq modeling of wave transformation, breaking, and runup. I: 1D. J. Waterw. Port Coast. Eng., *126*(1), 39–47. doi: 10.1061/(ASCE)0733-950X(2000)126:1(39)

Kilcher, L. F., and J. D. Nash. 2010. Structure and dynamics of the Columbia River tidal plume front. J. Geophys. Res. Oceans, *115*, C05S90. doi: 10.1029/2009JC006066

Kim, D.-H. 2015. H2D morphodynamic model considering wave, current and sediment interaction. Coast. Eng., *95*, 20–34. doi: 10.1016/j.coastaleng.2014.09.006

Kim, D.-H. and P. J. Lynett. 2011. Turbulent mixing and passive scalar transport in shallow flows. Phys. Fluids, *23*, 016603. doi: 10.1063/1.3531716

Kim, D.-H., and P. J. Lynett. 2013. A σ-coordinate transport model coupled with rotational boussinesq-type equations. Environ. Fluid Mech., *13*, 51–72. doi: 10.1007/s10652-012-9256-1

Kim, D.-H., P. J. Lynett, and S. A. Socolofsky. 2009. A depth-integrated model for weakly dispersive, turbulent, and rotational fluid flows. Ocean Model., *27*, 198–214. doi: 10.1016/j.ocemod.2009.01.005

Kirby, J. T. 2016. Boussinesq models and their application to coastal processes across a wide range of scales. J. Waterw. Port Coast Eng., *142*(6), 03116005. doi: 10.1061/(ASCE)WW.1943-5460.0000350

Kirby, J. T., and T.-M. Chen. 1989. Surface waves on vertically sheared flows: approximate dispersion relations. J. Geophys. Res. Oceans, *94*(C1), 1013–1027. doi: 10.1029/JC094iC01p01013

Kirby, J. T., and M. Derakhti. 2015. Turbulent bubbly flow under breaking waves. Presented at *13th U. S. National Congress on Computational Mechanics*, San Diego, CA.

Korteweg, D. J., and G. de Vries. 1895. On the change of form of long waves advancing in a rectangular canal, and on a new type of long stationary waves. Phil. Mag., *39*, 422–443. doi: 10.1080/14786449508620739

Kumar, N., G. Voulgaris, and J. C. Warner. 2011. Implementation and modification of a three-dimensional radiation stress formulation for surf zone and rip-current applications. Coast. Eng., *58*, 1097–1117. doi: 10.1016/j.coastaleng.2011.06.009

Kumar, N., G. Voulgaris, J. C. Warner, and M. Olabarrieta. 2012. Implementation of the vortex force formalism in the coupled ocean-atmosphere-wave-sediment transport (COAWST) modeling system for inner shelf and surf zone applications. Ocean Model., *47*, 65–95. doi: 10.1016/j.ocemod.2012.01.003

Kumar, N., F. Feddersen, Y. Uchiyama, J. McWilliams, and W. O'Reilly. 2015. Midshelf to surfzone coupled ROMS-SWAN model data comparison of waves, currents and temperature: diagnosis of subtidal forcings and response. J. Phys. Oceanogr., *45*, 1464–1490. doi: 10.1175/JPO-D-14-0151.1

Kumar, N., F. Feddersen, S. Suanda, Y. Uchiyama, and J. McWilliams. 2016. Mid- to inner-shelf coupled ROMS-SWAN model-data comparison of currents and temperature: diurnal and semidiurnal variability. J. Phys. Oceanogr., *46*, 841–862. doi: 10.1175/JPO-D-15-0103.1

Lakehal, D., and P. Liovic. 2011. Turbulence structure and interaction with steep breaking waves. J. Fluid Mech., *674*, 522–577. doi: 10.1017/jfm.2011.3

Lepelletier, T. G., and F. Raichlen. 1987. Harbor oscillations induced by nonlinear transient long waves. J. Waterw. Port Coast. Ocean Eng., *113*, 381–400. doi: 10.1061/(ASCE)0733-950X(1987)113:4(381)

Lesser, G. R., J. A. Roelvink, J. A. T. M. van Kester, and G. S. Stelling. 2004. Development and validation of a three-dimensional morphological model. Coast. Eng., *51*, 883–915. doi: 10.1016/j.coastaleng.2004.07.014

Li, N., V. Roeber, Y. Yamazaki, T. W. Heitmann, Y. Bai, and K. F. Cheung. 2014. Integration of coastal inundation modeling from storm tides to individual waves. Ocean Model., *83*, 26–42. doi: 10.1016/j.ocemod.2014.08.005

Lin, P., and P. L.-F. Liu. 1998. A numerical study of breaking waves in the surf zone. J. Fluid Mech., *359*, 239–264. doi: 10.1017/S002211209700846X

Longuet-Higgins, M. S. 1970a. Longshore currents generated by obliquely incident sea waves: 1. J. Geophys. Res.: Oceans Atmos., *75*(33), 6778–6789.

Longuet-Higgins, M. S. 1970b. Longshore currents generated by obliquely incident sea waves: 2. J. Geophys. Res.: Oceans Atmos., *75*(33), 6790–6801. doi: 10.1029/JC075i033p06790

Longuet-Higgins, M. S., and R. W. Stewart. 1960. Changes in the form of short gravity waves on long waves and tidal currents. J. Fluid Mech., *8*, 565–583. doi: 10.1017/S0022112060000803

Longuet-Higgins, M. S., and R. W. Stewart. 1962. Radiation stress and mass transport in gravity waves, with application to 'surf beats'. J. Fluid Mech., *12*, 481–504. doi: 10.1017/S0022112062000877

Longuet-Higgins, M. S., and R. W. Stewart. 1963. A note on wave set-up. J. Mar. Res., *21*, 4–10.

Longuet-Higgins, M. S., and R. W. Stewart. 1964. Radiation stresses in water waves; a physical discussion, with applications. Deep-Sea Res., *11*, 529–562. doi: 10.1016/0011-7471(64)90001-4

Lynett, P. J., J. A. Melby, and D.-H. Kim. 2010. An application of Boussinesq modeling to hurricane wave overtopping and inundation. Ocean Eng., *37*, 135–153.

Ma, G., F. Shi, and J. T. Kirby. 2011. A polydisperse two-fluid model for surf zone bubble simulation. J. Geophys. Res. Oceans, *116*, C05010. doi: 10.1029/2010JC006667

Ma, G., F. Shi, and J. T. Kirby. 2012. Shock-capturing non-hydrostatic model for fully dispersive surface wave processes. Ocean Model., *43–44*, 22–35. doi: 10.1016/j.ocemod.2011.12.002

Ma, G., J. T. Kirby, and F. Shi. 2013a. Numerical simulation of tsunami waves generated by deformable submarine landslides. Ocean Model., *69*, 146–165. doi: 10.1016/j.ocemod.2013.07.001

Ma, G., J. T. Kirby, S.-F. Su, J. Figlus, and F. Shi. 2013b. Numerical study of turbulence and wave damping induced by vegetation canopies. Coast. Eng., *80*, 68–78. doi: 10.1016/j.coastaleng.2013.05.007

Ma, G., Y.-J. Chou, and F. Shi. 2014. A wave-resolving model for nearshore suspended sediment transport. Ocean Model., *77*, 33–49. doi: 10.1016/j.ocemod.2014.03.003

Ma, G., J. T. Kirby, T.-J. Hsu, and F. Shi. 2015. A two-layer granular landslide model for tsunami wave generation: theory and computation. Ocean Model., *93*, 40–55. doi: 10.1016/j.ocemod.2015.07.012

McWilliams, J. C., J. M. Restrepo, and E. M. Lane. 2004. An asymptotic theory for the interaction of waves and currents in coastal waters. J. Fluid Mech., *511*, 135–178. doi: 10.1017/S0022112004009358

Mellor, G. 2003. The three-dimensional current and surface wave equations. J. Phys. Oceanogr., *33*, 1978–1989. doi: 10.1175/1520-0485(2003)033<1978:TTCASW>2.0.CO;2

Mellor, G. L. 2008. The depth-dependent current and wave interaction equations: a revision. J. Phys. Oceanogr., *38*, 2587–2596. doi: 10.1175/2008JPO3971.1

Monaghan, J. J., and A. Kos. 1999. Solitary waves on a Cretan beach. J. Waterw. Port Coast. Ocean Eng., *125*(3), 145–154. doi: 10.1061/(ASCE)0733-950X(1999)125:3(145)

Monismith, S. G. 2007. Hydrodynamics of coral reefs. Annu. Rev. Fluid Mech., *39*, 37–55. doi: 10.1146/annurev.fluid.38.050304.092125

Mulligan, R. P., A. E. Hay, and A. J. Bowen. 2010. A wave-driven jet over a rocky shoal. J. Geophys. Res.: Oceans, *115*, C10038. doi: 10.1029/2009JC006027

Newberger, P. A., and J. S. Allen. 2007. Forcing a three-dimensional, hydrostatic, primitive-equation model for application in the surf zone: 1. Formulation. J. Geophys. Res. Oceans, *112*, C08018. doi: 10.1029/2006JC003472

Nielsen, P., and D. P. Callaghan. 2003. Shear stress and sediment transport calculations for sheet flow under waves. Coast. Eng., *47*, 347–354. doi: 10.1016/S0378-3839(02)00141-2

Nwogu, O. 1993. Alternative form of Boussinesq equations for nearshore wave propagation. J. Waterw. Port Coast. Ocean Eng., *119*(6), 618–638. doi: 10.1061/(ASCE)0733-950X(1993)119:6(618)

Nwogu, O., and Z. Demirbilek. 2010. Infragravity wave motions and runup over shallow fringing reefs. J. Waterw. Port Coast. Ocean Eng., *136*(6), 295–305. doi: 10.1061/(ASCE)WW.1943-5460.0000050

Orzech, M. D., F. Shi, J. Veeramony, S. Bateman, J. Calantoni, and J. T. Kirby. 2016. Incorporating floating surface objects into a fully dispersive surface wave model. Ocean Model., *102*, 14–26. doi: 10.1016/j.ocemod.2016.04.007

Ozdemir, C. E., T.-J. Hsu, and S. Balachandar. 2011. A numerical investigation of lutocline dynamics and saturation of fine sediment in the oscillatory boundary layer. J. Geophys. Res. Oceans, *116*, C09012. doi: 10.1029/2011JC007185

Özkan-Haller, H. T., and J. T. Kirby. 1999. Nonlinear evolution of shear instabilities of the longshore current: A comparison of observations and computations. J. Geophys. Res. Oceans, *104*, 25953–25984. doi: 10.1029/1999JC900104

Özkan-Haller, H. T., and Y. Li. 2003. Effects of wave-current interaction on shear instabilities of longshore currents. J. Geophys. Res. Oceans, *108*(C5), 3139. doi: 10.1029/2001JC001287

Peregrine, D. H. 1967. Long waves on a beach. J. Fluid Mech., *27*, 815–827. doi: 10.1017/S0022112067002605

Peregrine, D. H. 1998. Surf zone currents. Theor. Comput. Fluid Dyn., *10*, 295–309. doi: 10.1007/s001620050065

Pizzo, N. E., and W. K. Melville. 2013. Vortex generation by deep-water breaking waves. J. Fluid Mech., *734*, 198–218. doi: 10.1017/jfm.2013.453

Putrevu, U., and I. A. Svendsen. 1999. Three-dimensional dispersion of momentum in wave-induced nearshore currents. Eur. J. Mech. B Fluids, pages 409–427. doi: 10.1016/S0997-7546(99)80038-7

Rego, V. S., J. T. Kirby, and D. Thompson. 2001. Boussinesq waves on vertically sheared currents. In: *Proceedings of the 4th International Symposium on Ocean Wave Measurement and Analysis*, WAVES 2001. B. L. Edge and J. M. Hemsley, eds. Reston, VA: American Society of Civil Engineers (ASCE); 904–913. doi: 10.1061/40604(273)92

Reniers, A. J. H. M., J. H. MacMahan, E. B. Thornton, T. P. Stanton, M. Henriquez, J. W. Brown, et al. 2009. Surf zone surface retention on a rip-channeled beach. J. Geophys. Res. Oceans, *114*, C10010. doi: 10.1029/2008JC005153

Reniers, A. J. H. M., J. H. MacMahan, F. J. Beron-Vera, and M. J. Olascoaga. 2010. Rip-current pulses tied to lagrangian coherent structures. Geophys. Res. Lett., *37*, L05605. doi: 10.1029/2009GL041443

Ribas, F., A. Falqués, H. E. de Swart, N. Dodd, R. Garnier, and D. Calvete. 2015. Understanding coastal morphodynamic patterns from depth-averaged sediment concentration. Rev. Geophys., *53*(2), 362–410.

Richard, G. L., and S. L. Gavrilyuk. 2013. The classical hydraulic jump in a model of shear shallow-water flows. J. Fluid Mech., *725*, 492–521. doi: 10.1017/jfm.2013.174

Richard, G. L., and S. L. Gavrilyuk. 2015. Modelling turbulence generation in solitary waves on shear shallow water flows. J. Fluid Mech., *773*, 49–74. doi: 10.1017/jfm.2015.236

Rijnsdorp, D. P., G. Ruessink, and M. Zijlema. 2015. Infragravity-wave dynamics in a barred coastal region, a numerical study. J. Geophys. Res. Oceans, *120*, 4068–4089. doi: 10.1002/2014JC010450

Roeber, V., and J. D. Bricker. 2015. Destructive tsunami-like wave generated by surf beat over a coral reef during Typhoon Haiyan. Nat. Commun., *6*(7854). doi: 10.1038/ncomms8854

Roeber, V., and K. F. Cheung. 2012. Boussinesq-type model for energetic breaking waves in fringing reef environments. Coast. Eng., *70*, 1–20. doi: 10.1016/j.coastaleng.2012.06.001

Roelvink, J. A. 2006. Coastal morphodynamic evolution techniques. Coast. Eng., *53*, 277–287. doi: 10.1016/j.coasaleng.2005.10.015

Roelvink, D., and A. Reniers. 2012. *A guide to modeling coastal morphology*, vol. 12, *Advances in Coastal and Ocean Engineering*. Singapore: World Scientific.

Romero, L., D. A. Siegel, J. C. McWilliams, Y. Uchiyama, and C. Jones. 2016. Characterizing storm water dispersion and dilution from small coastal streams. J. Geophys. Res. Oceans, *121*, 3926–3943. doi: 10.1002/2015JC011323

Ruessink, B. G., and Y. Kuriyama. 2008. Numerical predictability experiments of cross-shore sandbar migration. Geophys. Res. Lett., *35*, L01603. doi: 10.1029/2007GL032530

Ruessink, B. G., Y. Kuriyama, A. J. H. M. Reniers, J. A. Roelvink, and D. J. R. Walstra. 2007. Modeling cross-shore sandbar behavior on the timescale of weeks. J. Geophys. Res. Earth Surf., *112*, F03010. doi: 10.1029/2006JF000730

Schäffer, H. A., P. A. Madsen, and R. Deigaard. 1993. A Boussinesq model for waves breaking in shallow water. Coast. Eng., *20*, 185–202. doi: 10.1016/0378-3839(93)90001-O

Serre, F. 1953. Contribution à l'étude des écoulements permanents et variables dans les canaux. La Houille Blanche, *3*, 374–388. doi: 10.1051/lhb/1953034

Shen, C. 2001. Constituent Boussinesq equations for waves and currents. J. Phys. Oceanogr., *31*, 850–859. doi: 10.1175/1520-0485(2001)031<0850:NACCBE>2.0.CO;2

Shi, F., J. T. Kirby, and K. Haas. 2006. Quasi-3D nearshore circulation equations: a CL-vortex force formulation. In *Proceedings of the 30th International Conference on Coastal Engineering*, San Diego, J. M. Smith, ed. Singapore: World Scientific Publishing Co.; 1028–1039. doi: 10.1142/9789812709554_0088

Shi, F., J. T. Kirby, J. C. Harris, J. D. Geiman, and S. T. Grilli. 2012. A high-order adaptive time-stepping TVD solver for Boussinesq modeling of breaking waves and coastal inundation. Ocean Model., *43–44*, 36–51. doi: 10.1016/J.OCEMOD.2011.12.004

Shi, F., G. Vittori, and J. T. Kirby. 2015a. Concurrent correction method for modeling morphological response to dredging an offshore sandpit. Coast. Eng., *97*, 1–10. doi: 10.1016/j.costaleng.2014.12.008

Shi, J., F. Shi, J. T. Kirby, G. Ma, G. Wu, C. Tong et al. 2015b. Pressure decimation and interpolation (PDI) method for a baroclinic non-hydrostatic model. Ocean Model., *96*, 265–279. doi: 10.1016/j.ocemod.2015.09.010

Skop, R. A. 1987. Approximate dispersion relation for wave-current interactions. J. Waterw. Port Coast. Ocean Eng., *113*, 187–195. doi: 10.1061/(ASCE)0733-950X(1987)113:2(187)

Sleath, J. F. A. 1999. Conditions for plug flow formation in oscillatory flow. Cont. Shelf Res., *19*, 1643–1664. doi: 10.1016/S0278-4343(98)00096-X

Slinn, D. N., J. S. Allen, P. A. Newberger, and R. A. Holman. 1998. Nonlinear shear instabilities of alongshore currents over barred beaches. J. Geophys. Res. Oceans, *103*, 18357–18379. doi: 10.1029/98JC01111

Smit, M. W. J., A. J. H. M. Reniers, and M. J. F. Stive. 2012. Role of morphological variability in the evolution of nearshore sandbars. Coast. Eng., *69*, 19–28. doi: 10.1016/j.coastaleng.2012.05.005

Smit, P., M. Zijlema, and G. Stelling. 2013. Depth-induced wave breaking in a non-hydrostatic, near-shore wave model. Coast. Eng., *76*, 1–16. doi: 10.1016/j.coastaleng.2013.01.008

Smit, P., T. Janssen, L. Holthuijsen, and J. Smith. 2014. Non-hydrostatic modeling of surf zone wave dynamics. Coast. Eng., *83*, 36–48. doi: 10.1016/j.coastaleng.2013.09.005

Smit, P. B., T. T. Janssen, and T. H. C. Herbers. 2015. Stochastic modeling of inhomogeneous ocean waves. Ocean Model., *96*, 26–35. doi: 10.1016/j.ocemod.2015.06.009

Smith, J. A. 2006. Wave-current interactions in finite depth. J. Phys. Oceanogr., *36*, 1403–1419. doi: 10.1175/JPO2911.1

Smith, R. 1995. Multi-mode models of flow and of solute dispersion in shallow water. Part 1. General derivation. J. Fluid Mech., *283*, 231–248. doi: 10.1017/S0022112095002291

Son, S., and P. J. Lynett. 2014. Interaction of dispersive water waves with weakly sheared currents of arbitary profile. Coast. Eng., *90*, 64–84. doi: 10.1016/j.coastaleng.2014.04.009

Spydell, M., and F. Feddersen. 2009. Lagrangian drifter dispersion in the surf zone: Directionally spread, normally incident waves. J. Phys. Oceanogr., *39*, 809–830.

Stelling, G. S., and M. Zijlema. 2003. An accurate and efficient finite-difference algorithm for non-hydrostatic free-surface flow with application to wave propagation. Int. J. Numer. Methods Fluids, *43*, 1–23. doi: 10.1002/fld.595

Stewart, R. H., and J. W. Joy. 1974. HF radio measurements of surface currents. Deep Sea Res., *21*, 1039–1049. doi: 10.1016/0011-7471(74)90066-7

Stive, M. J. F., and H. J. De Vriend. 1994. Shear stresses and mean flow in shoaling and breaking waves. In *Proceedings of the 24th International Conference on Coastal Engineering*, Kobe, Japan. B. L. Edge, ed. Reston, VA: American Society of Civil Engineers (ASCE); 594–608.

Suanda, S. H., and F. Feddersen. 2015. A self-similar scaling for cross-shelf exchange driven by transient rip currents. Geophys. Res. Lett., *42*, 5427–5434. doi: 10.1002/2015GL063944

Sullivan, P. P., J. C. McWilliams, and W. K. Melville. 2007. Surface gravity wave effects in the oceanic boundary layer: large-eddy simulation with vortex force and stochastic breakers. J. Fluid Mech., *593*, 405–452. doi: 10.1017/S002211200700897X

Svendsen, I. A., and U. Putrevu. 1994. Nearshore mixing and dispersion. Proc. R. Soc. Lond. A Math. Phys. Sci., *445*(1925), 561–576. doi: 10.1098/rspa.1994.0078

Taylor, G. 1953. Dispersion of soluble matter in solvent flowing slowly through a tube. Proc. R. Soc. Lond. A Math. Phys. Sci., *219*(1137), 186–203. doi: 10.1098/rspa.1953.0139

Thornton, E. B., and R. T. Guza. 1983. Transformation of wave height distribution. J. Geophys. Res. Oceans, *88*(C10), 5925–5938. doi: 10.1029/JC088iC10p05925

Ting, F. C. K., and J. Reimnitz. 2015. Volumetric velocity measurements of turbulent coherent structures induced by plunging regular waves. Coast. Eng., *104*, 93–112. doi: 10.1016/j.coastaleng.2015.07.002

Tissier, M., P. Bonneton, F. Marche, F. Chazel, and D. Lannes. 2012. A new approach to handle wave breaking in fully non-linear Boussinesq models. Coast. Eng., *67*, 54–66. doi: 10.1016/j.coastaleng.2012.04.004

Tonelli, M., and M. Petti. 2009. Hybrid finite volume-finite difference scheme for 2DH improved Boussinesq equations. Coast. Eng., *56*, 609–620. doi: 10.1016/j.coastaleng.2009.01.001

Tonelli, M., and M. Petti. 2010. Finite volume scheme for the solution of 2D extended Boussinesq equations in the surf zone. Ocean Eng., *37*, 567–582. doi: 10.1016/j.oceaneng.2010.02.004

Tonelli, M., and M. Petti. 2011. Simulation of wave breaking over complex bathymetries by a Boussinesq model. J. Hydraul. Res., *49*(4), 473–486. doi: 10.1080/00221686.2010.538570

Tonelli, M., and M. Petti. 2012. Shock-capturing Boussinesq model for irregular wave propagation. Coast. Eng., *61*, 8–19. doi: 10.1016/j.coastaleng.2011.11.006

Toro, E. F. 2001. *Shock-capturing methods for free-surface shallow flows*. Hoboken, NJ: John Wiley & Sons, Ltd.

Uchiyama, Y., J. C. McWilliams, and J. M. Restrepo. 2009. Wave-current interaction in nearshore shear instability analyzed with a vortex force formalism. J. Geophys. Res. Oceans, *114*, C06021. doi: 10.1029/2008JC005135

Uchiyama, Y., J. C. McWilliams, and A. F. Shchepetkin. 2010. Wave-current interaction in an oceanic circulation model with a vortex-force formalism: application to the surf zone. Ocean Model., *34*, 16–35. doi: 10.1016/j.ocemod.2010.04.002

van der Wegen, M., and J. A. Roelvink. 2008. Long-term morphodynamic evolution of a tidal embayment using a two-dimensional, process-based model. J. Geophys. Res. Oceans, *113*, C03016. doi: 10.1029/2006JC003983

van der Wegen, M., Z. B. Wang, H. H. G. Savenije, and J. A. Roelvink. 2008. Long-term morphodynamic evolution and energy dissipation in a coastal plain, tidal embayment. J. Geophys. Res. Earth Surf., *113*, F03001. doi: 10.1029/2007JF000898

Van Dongeren, A., J. A. Battjes, T. Janssen, J. van Noorloos, K. Steenauer, G. Steenbergen et al. 2007. Shoaling and shoreline dissipation of low-frequency waves. J. Geophys. Res. Oceans, *112*, C02011. doi: 10.1029/2006JC003701

van Reeuwijk, M., 2002. Efficient simulation of non-hydrostatic free-surface flow. Master's (M.Sc.) thesis. Delft University of Technology.

Veeramony, J., and I. A. Svendsen. 2000. The flow in surf-zone waves. Coast. Eng., *39*, 93–122. doi: 10.1016/S0378-3839(99)00058-7

Walstra, D. J. R., B. G. Ruessink, A. J. H. M. Reniers, and R. Ranasinghe. 2015. Process-based modeling of kilometer-scale alongshore sandbar variability. Earth Surf. Processes Landforms, *40*, 995–1005. doi: 10.1002/esp.3676

Warner, J. C., N. Perlin, and E. D. Skyllingstad. 2008. Using the model coupling toolkit to couple earth system models. Environ. Model Softw., *23*, 1240–1249. doi: 10.1016/j.envsoft.2008.03.002

Warner, J. C., B. Armstrong, R. He, and J. B. Zambon. 2010. Development of a coupled ocean-atmosphere-wave-sediment transport (COAWST) modeling system. Ocean Model., *35*, 230–244. doi: 10.1016/j.ocemod.2010.07.010

Wei, G., J. T. Kirby, S. T. Grilli, and R. Subramanya. 1995. A fully nonlinear Boussinesq model for surface waves. Part 1. Highly nonlinear unsteady waves. J. Fluid Mech., *294*, 71–92. doi: 10.1017/S0022112095002813

Weir, B., Y. Uchiyama, E. M. Lane, J. M. Restrepo, and J. C. McWilliams. 2011. A vortex force analysis of the interaction of rip currents and surface gravity waves. J. Geophys. Res. Oceans, *116*, C05001. doi: 10.1029/2010JC006232

Wu, W.-C., G. Ma, and D. T. Cox. 2016. Modeling wave attenuation induced by the vertical density variations of vegetation. Coast. Eng., *112*, 17–27. doi: 10.1016/j.coastaleng.2016.02.004

Xiao, H., Y. Young, and J. Prévost. 2010. Hydro- and morpho-dynamic modeling of breaking solitary waves over a fine sand beach. Part II: Numerical simulation. Mar. Geol., *269*, 119–131. doi: 10.1016/j.margeo.2009.12.008

Yoon, S. B., and P. L.-F. Liu. 1989. Interactions of currents and weakly nonlinear water waves in shallow water. J. Fluid Mech., *205*, 397–419. doi: 10.1017/S0022112089002089

Yoon, S. B., and P. L.-F. Liu. 1990. Effects of opposing waves on momentum jets. J. Waterw. Port Coast. Ocean Eng., *116*(5), 545–557. doi: 10.1061/(ASCE)0733-950X(1990)116:5(545)

Young, C.-C., C. H. Wu, J.-T. Kuo, and W.-C. Liu. 2007. A higher-order σ-coordinate non-hydrostatic model for nonlinear surface waves. Ocean Eng., *34*, 1357–1370. doi: 10.1016/j.oceaneng.2006.11.001

Yu, J., and D. N. Slinn. 2003. Effects of wave-current interaction on rip currents. J. Geophys. Res. Oceans, *108*(C3), 3088. doi: 10.1029/2001JC001105

Yuan, H., and C. H. Wu. 2004. An implicit three-dimensional fully non-hydrostatic model for free-surface flows. Int. J. Numer. Methods Fluids, *46*, 709–733. doi: 10.1002/fld.778

Zelt, J. A. 1991. The run-up of nonbreaking and breaking solitary waves. Coast. Eng., *15*, 205–246. doi: 10.1016/0378-3839(91)90003-Y

Zijlema, M., and G. S. Stelling. 2008. Efficient computation of surf zone waves using the non-linear shallow water equations with non-hydrostatic pressure. Coast. Eng., *55*, 780–790. doi: 10.1016/j.coastaleng.2008.02.020

Zijlema, M., G. Stelling, and P. Smit. 2011. SWASH: an operational public domain code for simulating wave fields and rapidly varied flows in coastal waters. Coast. Eng., *58*, 992–1012. doi: 10.1016/j.coastaleng.2011.05.015

Received: *4 May 2016*; revised: *31 January 2017*.

Editor's note: Contributions to *The Sea: The Science of Ocean Prediction* are being published separately in special issues of *Journal of Marine Research* and will be made available in a forthcoming supplement as Volume 17 of the series.